J|A|C|S
ARTICLES
Published on Web 02/08/2007

Reactions of Monomeric [1,2,4-$(Me_3C)_3C_5H_2]_2CeH$ and CO with or without H_2: An Experimental and Computational Study

Evan L. Werkema,[†] Laurent Maron,*[,‡,§] Odile Eisenstein,*[,||] and Richard A. Andersen*[,†]

Contribution from the Chemistry Department and Chemical Sciences Division of Lawrence Berkeley National Laboratory, University of California, Berkeley, California 94720, Laboratoire de Physique Quantique, (UMR 5626-CNRS), IRSAMC, Université Paul Sabatier, 118 Route de Narbonne, 31064 Toulouse Cedex 04, France, and Institut Charles Gerhardt (UMR 5253-CNRS-UM2-ENSCM-UM1), Chimie Théorique, Méthodologies, Modélisations, Université Montpellier 2, 34095 Montpellier, France

Received September 7, 2006; E-mail: laurent.maron@irsamc.ups-tlse.fr; odile.eisenstein@univ-montp2.fr; raandersen@lbl.gov

Abstract: Addition of CO to $[1,2,4\text{-}(Me_3C)_3C_5H_2]_2CeH$, Cp'_2CeH, in toluene yields the *cis*-$(Cp'_2Ce)_2(\mu\text{-}OCHCHO)$, in which the *cis*-enediolate group bridges the two metallocene fragments. The *cis*-enediolate quantitatively isomerizes intramolecularly to the *trans*-enediolate in C_6D_6 at 100 °C over 7 months. When the solvent is pentane, $Cp'_2Ce(OCH_2)CeCp'_2$ forms, in which the oxomethylene group or the formaldehyde dianion bridges the two metallocene fragments. The *cis*-enediolate is suggested to form by insertion of CO into the Ce−C bond of $Cp'_2Ce(OCH_2)CeCp'_2$, generating $Cp'_2CeOCH_2COCeCp'_2$. The stereochemistry of the *cis*-enediolate is determined by a 1,2-hydrogen shift in the OCH_2CO fragment that has the $OC(H_2)$ bond anti-periplanar relative to the carbene lone pair. The bridging oxomethylene complex reacts with H_2, but not with CH_4, to give Cp'_2CeOMe, which is also the product of the reaction between Cp'_2CeH and a mixture of CO and H_2. The oxomethylene complex reacts with CO to give the *cis*-enediolate complex. DFT calculations on C_5H_5 model metallocenes show that the reaction of Cp_2CeH with CO and H_2 to give Cp_2CeOMe is exoergic by 50 kcal mol^{-1}. The net reaction proceeds by a series of elementary reactions that occur after the formyl complex, $Cp_2Ce(\eta^2\text{-}CHO)$, is formed by further reaction with H_2. The key point that emerges from the calculated potential energy surface is the bifunctional nature of the metal formyl in which the carbon atom behaves as a donor and acceptor. Replacing H_2 by CH_4 increases the activation energy by 17 kcal mol^{-1}.

Introduction

Hydrogenation of carbon monoxide to methanol and higher alcohols is an industrially important and an academically interesting reaction.[1] The formation of methanol from carbon monoxide and hydrogen is exothermic by 6 kcal mol^{-1} [2] but endoergic at 500 K, where $\Delta G = +5$ kcal mol^{-1}.[3] The industrial reaction is catalyzed by Cu/ZnO and the heterogeneous reaction has been intensively studied.[4] Organometallic hydride compounds have been studied as models to gain information about the energetics of the elementary reactions that comprise the net reaction.[5−7] Reaction of early d- and f-transition metal hydrides with carbon monoxide are postulated to form metal formyl species, which react further with either dihydrogen or carbon monoxide to yield the isolated products. Thus, $(C_5Me_5)_2ZrH_2$ reacts with CO forming the adduct, $(C_5Me_5)_2Zr(H)_2(CO)$, at low-temperature that yields *trans*-$[(C_5Me_5)_2Zr(H)]_2(\mu\text{-}OCH{=}CHO)$ on warming. When the adduct is warmed under H_2, $(C_5Me_5)_2Zr(H)(OMe)$, and $(C_5Me_5)_2Zr(CO)_2$ are formed.[8] In contrast, the *cis*-enediolate, *cis*-$[(C_5Me_5)_2Zr(H)]_2(\mu\text{-}OCH{=}CHO)$ is the sole product formed when $(C_5Me_5)_2ZrH_2$ and $(C_5Me_5)_2Zr(CO)_2$ are mixed in presence of H_2.[9] The hafnium metallocene behaved similarly, although it was noted that the cis- and trans-

[†] University of California.
[‡] Université Paul Sabatier.
[§] Present address: Laboratoire de Nanophysique, Magnétisme et Optoéléctronique, INSA, 135 avenue de Rangueil, 31077, Toulouse Cedex, France.
[||] Université Montpellier 2.

(1) Ponec, V. *Catal. Rev. Sci. Eng.* **1978**, *18*, 151. Masters, C. *Adv. Organomet. Chem.* **1979**, *17*, 61. Kung, H. H. *Catal. Rev. Sci. Eng.* **1980**, *22*, 235. Klier, K. *Adv. Cat.* **1982**, *31*, 243. Dombeck, B. D. *Adv. Cat.* **1983**, *32*, 325. Muetterties, E. L.; Stein, J. *Chem. Rev.* **1979**, *79*, 479. Rofer-DePoorter, C. K. *Chem. Rev.* **1981**, *81*, 447.
(2) Lewis, G. N.; Randall, M. *Thermodynamics*; Revised by Pitzer, K. S.; Brewer, L.; McGraw-Hill: New York, 1961.
(3) Stull, D. R.; Westrum, E. F., Jr.; Sinke, G. C. *The Thermodynamic of Organic Compounds*; Wiley: New York, N. Y. 1969.
(4) For a recent study, see Jones, P. M.; May, J. A.; Reitz, J. B.; Solomon, E. I. *Inorg. Chem.* **2004**, *43*, 3349. Cotton F. A.; Wilkinson, G. *Advanced Inorganic Chemistry*, 5th ed.; Wiley: New York, 1988; pp 1228.
(5) Wolczanski, P. T.; Bercaw, J. E. *Acc. Chem. Res.* **1980**, *13*, 121.
(6) Erker, G. *Acc. Chem. Res.* **1984**, *17*, 103. Gladysz, J. A. *Adv. Organomet. Chem.* **1982**, *20*, 1. Jordan, R. F. *Adv. Organomet. Chem.* **1991**, *32*, 325. Durfee, L. D.; Rothwell, I. P. *Chem. Rev.* **1988**, *88*, 1059. Kahn, B. E.; Rieke, R. D. *Chem. Rev.* **1988**, *88*, 733. Fachinetti, G.; Floriani, C.; Roselli, A.; Pucci, S. *J. Chem. Soc. Chem. Commun.* **1978**, 269. Fandos, R.; Fierro, J. L. G.; Kubicki, M. M.; Otero, A.; Terreros, P.; Vivar-Cerrato, M. A. *Organometallics* **1995**, *14*, 2162.
(7) Fagan, P. J.; Moloy, K. G.; Marks, T. J. *J. Am. Chem. Soc.* **1981**, *103*, 6959.
(8) Manriquez, J. M; McAlister, D. R.; Sanner, R. D.; Bercaw, J. E. *J. Am. Chem. Soc.* **1978**, *100*, 2716.
(9) Wolczanski, P. T.; Threlkel, R. S.; Bercaw, J. E. *J. Am. Chem. Soc.* **1979**, *101*, 218.

endiolates are formed and the cis−trans ratio was always greater than unity.[10] The amide hydride, $[(Me_3C)_3SiN(H)]_3ZrH$, reacts with excess CO to yield the cis-enediolate, $\{[(Me_3C)_3SiN(H)]_3Zr\}_2(\mu\text{-}OCH{=}CHO)$.[11] In this case, an η^2-formaldehyde complex $\{[(Me_3C)_3SiN(H)]_3Zr\}_2(\mu\text{-}OCH_2)$ was isolated and shown to be an intermediate, because it reacts with CO to yield the enediolate by way of the CO insertion species, $\{[(Me_3C)_3SiN(H)]_3Zr\}_2(\mu\text{-}OCH_2CO)$, which was detected spectroscopically. The η^2-formaldehyde complex does not react with dihydrogen, but it thermally decomposes to $[(Me_3C)_3SiN(H)]_3ZrOMe$ and $[(Me_3C)_3SiN(H)]_2Zr{=}NSi(CMe_3)_3$. The samarium hydride, $(C_5Me_5)_4Sm_2(\mu\text{-}H)_2$, reacts with CO to give the *cis*- and *trans*-enediolate complexes, $[(C_5Me_5)_2Sm]_2(\mu\text{-}OCH{=}CHO)$, which were isolated as their Ph_3PO adducts. It was shown that the *cis*-enediolate isomerizes to the *trans*-enediolate though the isomerism mechanism was not studied.[12a] The dimeric ytterbium hydride, [tris(3-Me_3C-5-Me-pyrazolyl)-borate]$_2Yb_2(\mu\text{-}H_2)_2$ gives the *cis*-enediolate on reaction with CO, $[Pz'_3BH)Yb]_2(\mu\text{-}OCH{=}CHO)$.[12b] Recently, the tetrameric yttrium and lutetium dihydrides, $[(Me_3Si)(Me)_4C_5]_4M_4(\mu\text{-}H)_8(thf)$, were found to yield $[(Me_3Si)(Me)_4C_5]_4M_4(\mu\text{-}O)$ on reaction with CO and ethylene; in the case of M = Y, oxomethylene complexes were isolated and characterized.[12c] The monomeric metallocenes of thorium, $(C_5Me_5)_2Th(H)(OR)$, where R = $CH(CMe_3)_2$ or 2,6-$(Me_3C)_2C_6H_4$, reacts reversibly with CO at low temperature to give a formyl, $(C_5Me_5)_2Th(CHO)(OR)$, which is spectroscopically detected but not isolated, that reacts with additional CO to give the isolable cis-enediolate, $[(C_5Me_5)_2Th(OR)]_2(\mu\text{-}OCH{=}CHO)$.[7] The initial insertion step follows second-order kinetics with an activation free energy, $\Delta G^{\ddagger}$ (−50 °C), of 9.2 kcal mol^{-1} and the formation of the formyl is exoergic, because ΔG (−50 °C) is −1.8 kcal mol^{-1}.[13] When a mixture of H_2 and CO (60:1) is used, the methoxide, $(C_5Me_5)_2Th(OMe)(OR)$, forms presumably due to the trapping of the formyl complex by dihydrogen.

In this paper, reaction of the monomeric cerium hydride $[1,2,4\text{-}(Me_3C)_3C_5H_2]_2CeH$[14] with a mixture of hydrogen and carbon monoxide to give quantitatively $[1,2,4\text{-}(Me_3C)_3C_5H_2]_2CeOMe$ is described. When H_2 is absent, other carbonylation products are formed, some of which are converted to the methoxide with H_2. The mechanism of the hydrogenation reaction is explored by DFT calculations, which illuminate the energetics of the elementary steps involved in the net reaction.

Results

Experimental Studies. Addition of carbon monoxide to a purple solution of $[1,2,4\text{-}(Me_3C)_3C_5H_2]_2CeH$, abbreviated as Cp'_2CeH, dissolved in toluene yields a red solution instantaneously from which the red enediolate, **1**, may be isolated by

Scheme 1. Net Reactions of Cp'_2CeH (Cp′ = 1,2,4-tri-*t*-butylcyclopentadienyl)

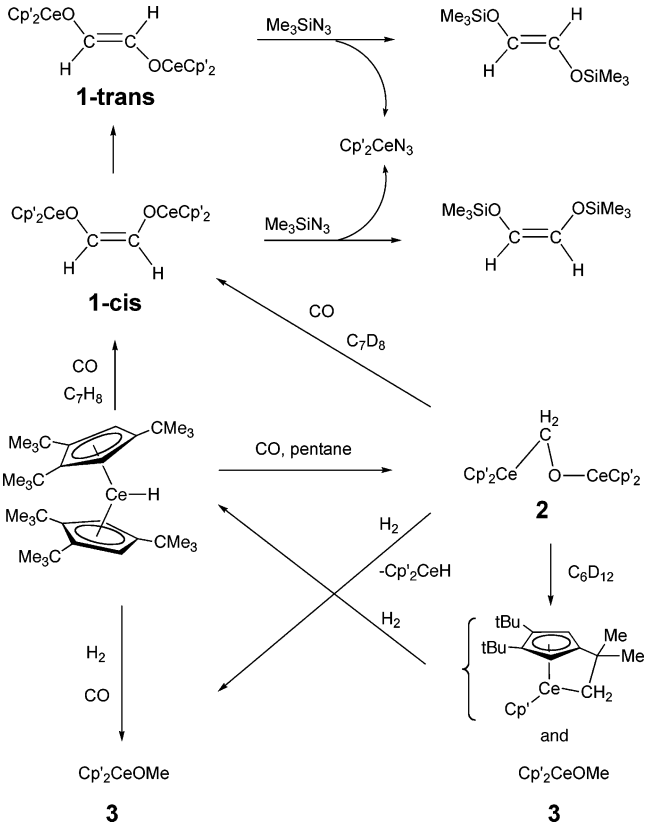

crystallization from pentane, Scheme 1. The solid melts at 232−235 °C and gives a molecular ion in the mass spectrum. The ^{1}H NMR spectrum at 20 °C in C_6D_6 is consistent with formation of an enediolate complex but the chemical shift pattern does not distinguish between the cis- and trans-stereoisomers. Single crystals grown by sublimation (see below) are small and weakly diffracting, but a data set was collected using synchrotron radiation, see Experimental Section and Supporting Information for details. The ORTEP diagram shown in Figure 1a shows that the stereochemistry of the enediolate fragment is cis; therefore, **1-cis** is the initial product formed, Scheme 1; important bond distances and angles are listed in the figure captions.

In solution (C_6D_6), the ^{1}H NMR resonances of **1-cis** slowly diminish as new ones appear over a period of months; the number of resonances is conserved but their chemical shifts are different. The transformation is complete after heating a C_7D_8 solution at 100 °C over 7 months; the half-life is about 2 months and the total intensity of the initial Me_3C resonances decreases by about 20% during this time period. The rearrangement also occurs in the solid state. Heating solid **1-cis** in a sealed ampule at 190 °C under static vacuum for two weeks results in formation of orange and red crystals, with different crystalline morphologies, on the cool (20°) walls of the ampule. These crystals can be separated manually and the orange crystals have the same space group and unit cell parameters as observed for the **1-cis**. The red crystals crystallize in the same space group as the orange crystals, $P\bar{1}$, but have different unit cell dimensions. An ORTEP diagram is shown in Figure 1b; an inversion center is located midway between the carbon−carbon double bond, C35−C35_2, which defines the stereochemistry of the molecule as trans, **1-trans**.

(10) Roddick, D. M.; Fryzuk, M. D.; Seidler, P. F.; Hillhouse, G. L.; Bercaw, J. E. *Organometallics* **1985**, *4*, 97. Corrections *Organometallics* **1985**, *4*, 1694.
(11) Cummins, C. C.; Van Duyne, G. D.; Schaller, C. P.; Wolczanski, P. T. *Organometallics* **1991**, *10*, 164.
(12) (a) Evans, W. J.; Grate, J. W.; Doedens, R. J. *J. Am. Chem. Soc.* **1985**, *107*, 1671. (b) Ferrence, G. M.; McDonald, R.; Takats, J. *Angew. Chem. Int. Ed.* **1999**, *38*, 2233. (c) Shima, T.; Hou, Z. *J. Am. Chem. Soc.* **2006**, *128*, 8124.
(13) Moloy, K. G.; Marks, T. J. *J. Am. Chem. Soc.* **1984**, *106*, 7051.
(14) (a) Maron, L.; Werkema, E. L.; Perrin, L.; Eisenstein, O.; Andersen, R. A. *J. Am. Chem. Soc.* **2005**, *127*, 279. (b) Werkema, E. L.; Messines, E.; Perrin, L.; Maron, L.; Eisenstein, O. Andersen, R. A. *J. Am. Chem. Soc.* **2005**, *127*, 7781.

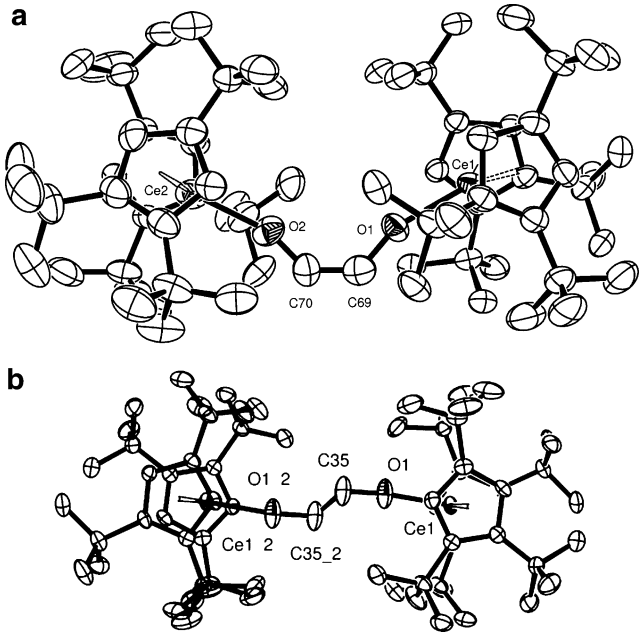

Figure 1. (a) ORTEP diagram of *cis*-1,2-[(1,2,4-$(Me_3C)_3C_5H_2)_2CeO]_2C_2H_2$, **1-cis**. (50% probability ellipsoids), the non-hydrogen atoms were refined anisotropically and all the hydrogen atoms were placed (but not shown) in calculated positions; Ce−C(ave.) = 2.83 ± 0.02 Å, Ce−Cp′(ring perpendicular) = 2.53 Å (ave.), Ce(1)−O(1) = 2.173(4) Å, Ce(2)−O(2) = 2.170(5) Å, O(1)−C(69) = 1.382(8) Å, O(2)−C(70) = 1.351(8) Å, C(69)−C(70) = 1.32(1) Å, Ce(1)−O(1)−C(69) = 159.6(4)°, Ce(2)−O(2)−C(70) = 160.0(5)°, O(1)−C(69)−C(70) = 129.1(7)°, O(2)−C(70)−C(69) = 135.2(7)°, O(1)−C(69)−C(70)−O(2) torsion angle = 7.9(15)°, Cp′(ring perpendicular)−Ce−Cp′(ring perpendicular) = 143.4° (ave.). (b) ORTEP diagram of *trans*-1,2-[(1,2,4-$(Me_3C)_3C_5H_2)_2CeO]_2C_2H_2$, **1-trans**. (50% probability ellipsoids), the non-hydrogen atoms were refined anisotropically and all the hydrogen atoms were placed (but not shown) in calculated positions; Ce−C(ave.) = 2.83 ± 0.02 Å, Ce−Cp(ring centroid) (ave.) = 2.56 Å, Ce(1)−O(1) = 2.118(3) Å, O(1)−C(35) = 1.352(5) Å, C(35)−C(35_2) = 1.28(1) Å, Ce(1)−O(1)−C(35) = 165.5(3)°, O(1)−C(35)−C(35_2) = 124.9(7)°, Cp′(ring centroid)−Ce−Cp′(ring centroid) = 153(9)°.

The orientation of the Cp'_2CeO fragments in **1-cis** and **1-trans** is anti, relative to the C−C double bond, with a Ce−O−C(olefinic) angle of 159.8(1) (ave.) and 165.5(3)°, respectively. The cyclopentadienyl rings have different orientations in the two isomers, but the averaged Ce−C distances are identical, as are the O−C and C−C distances. The bond distances in the enediolate fragment are similar to those found in the cis and trans isomers of $[(C_5Me_5)_2(Ph_3PO)Sm]_2(\mu$-OCH═CHO).[12a] The C−C distances of 1.32(1) and 1.28(1) Å are slightly shorter than the average distance found for the $C{=}CO^{(-)}$ fragment of 1.36 Å, and the C−O distances of 1.366(8) and 1.352(5) Å are slightly longer than that found in the $C{=}CO^{(-)}$ fragment of 1.33 Å.[15] The principle structural difference between the isomers is that the Ce−O distance of 2.171(1) Å in **1-cis** is longer than that of 2.118(3) Å in **1-trans**. The latter distance is identical to that found for the averaged terminal Ce−O distance of 2.120(2) Å in $(C_5Me_5)_2Ce_2(OCMe_3)_2(\mu$-$OCMe_3)_2$[16a] but shorter than that found in $(C_5Me_5)_2Ce(O$-2,6-$(Me_3C)_2C_6H_3)$ of 2.248(2) Å.[16b]

The initial ^{1}H NMR spectrum that appears on mixing Cp'_2CeH with CO in C_6D_6 is shown to be due to **1-cis** in the following manner. In an NMR tube containing **1**, addition of an excess of Me_3SiN_3 to the solution of the enediolate results in disappearance of the resonances due to **1** and formation of resonances due to Cp'_2CeN_3, see Experimental Section for synthetic and characterization details, and *cis*-1,2-$(Me_3SiO)_2C_2H_2$. The cis-stereochemistry of the latter is shown by comparison of the chemical shift of the olefinic C−H group to that of an authentic specimen.[17] Similarly, addition of Me_3SiN_3 to an NMR tube containing the rearranged enediolate results in the appearance of resonances due to Cp'_2CeN_3 and the olefinic resonance of *trans*-1,2-$(Me_3SiO)_2C_2H_2$.[17] In addition, hydrolysis (H_2O) of each sample and analysis by GCMS showed one volatile compound (excluding solvent and Cp′H) that exhibited a M^+ of 204 amu, which identifies it as bis(trimethylsiloxy)ethylene. Further, hydrolysis of a mixture of **1-cis** and **1-trans** and analysis by GCMS showed that both isomers of 1,2-$(Me_3SiO)_2C_2H_2$ are present in varying amounts as a function of time. Thus, the initially formed enediolate is **1-cis**, and it isomerizes to **1-trans** over time, Scheme 1. The isolated amount of pure **1-trans** is small and no physical properties, other than its ^{1}H NMR spectrum and crystal structure, are available at this time.The enediolate **1-cis** has average C_{2v} symmetry in the solid state and the 20 °C ^{1}H NMR spectrum consists of four relatively broadened resonances that are due to the CH groups on the enediolate fragment and ring CH's on the cyclopentadienyl rings at $\delta = 39$ and $\delta = 27$, respectively, and two Me_3C resonances in a 2:1 area ratio at $\delta = -0.73$ and $\delta = 12.5$ ppm. As the temperature is decreased, the resonances due to the ring CH's broaden and disappear and the Me_3C resonance of area 2 broadens and decoalesces, $\Delta G^{\ddagger}(T_c = 0°) = 11$ kcal mol^{-1}, which is shown in a δ vs $1/T$ plot in Figure 2. As the temperature is decreased further, the three equal-area Me_3C-resonances broaden and by −70 °C, they appear as six equal area resonances, implying that the Cp′ rings on each metallocene fragment are chemically inequivalent but the C_2-axis remains. The molecule is clearly fluxional and a physical process that accounts for the fluxional motion is oscillation or hindered rotation of the cyclopentadienyl rings about their pseudo-C_5 axes that is slow at −70 °C so that the six Me_3C-groups are inequivalent. As the temperature is increased, the Cp′ ring oscillation increases and, on time average, the top and bottom rings of the bent metallocene fragments become equivalent resulting in a 2:2:2 pattern. As the temperature is increased further, the rate of rotation of the substituted cyclopentadienyl rings about their pseudo-C_5 axes increases, resulting in the creation of a time-average horizontal mirror plane of symmetry, which exchanges two of the three Me_3C-sites.

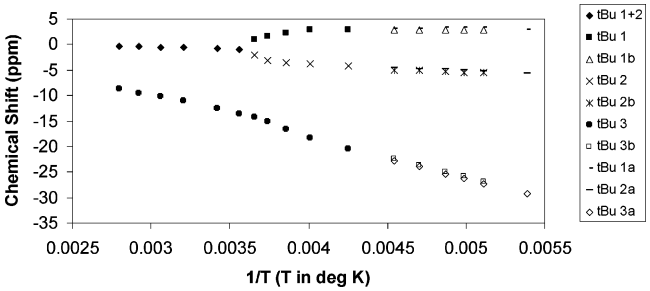

Figure 2. Chemical shift vs $1/T$ for **1-cis**.

(15) Allen, F. H.; Kennard, O.; Watson; D. G.; Brammer, L.; Orpen, A. G.; Taylor, R. *J. Chem Soc. Perkin Trans. II* **1987**, S1.
(16) (a) Heeres, H. J.; Teuben, J. H.; Rogers, R. D. *J. Organomet. Chem.* **1989**, *364*, 87. (b) Heeres, H. J.; Meetsma, A.; Teuben, J. H. *J. Chem. Soc. Chem. Commun.* **1988**, 962.
(17) Scharf, H. D.; Mattay, J. *Tetrahedron Lett.* **1976**, *39*, 3509.

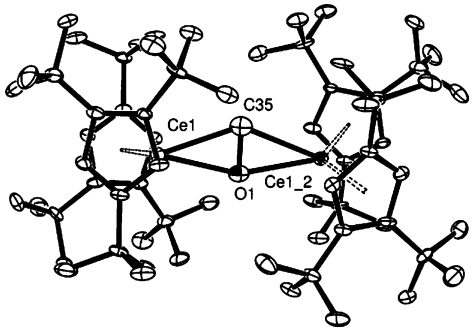

Figure 3. ORTEP diagram for $[(1,2,4\text{-}(Me_3C)_3C_5H_2)_2Ce]_2(\mu\text{-}OCH_2)$, **2**. (50% probability ellipsoids); the toluene of crystallization is not shown. The non-hydrogen atoms except C(35) were refined anisotropically and the hydrogen atoms were placed (but not shown) in calculated positions. Ce(1)−C(ave) = 2.86 ± 0.05 Å, Ce−Cp′(ring perpendicular) = 2.59 Å (ave.) Ce(1)−O(1) = 2.443(2) Å, Ce(1)−C(35) = 2.554(4) Å, C(35)−O(1) = 1.39(1) Å, C(35)−Ce(1)−O(1) = 32.2(3)°, Cp′(ring perpendicular)−Ce−Cp′(ring perpendicular) = 135°.

Chart 1

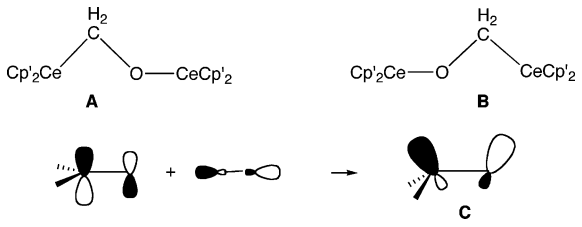

When carbon monoxide is added to a solution of Cp'_2CeH in pentane, a yellow precipitate forms (Scheme 1). The yellow solid dissolves in toluene from which it crystallizes as orange prisms, **2**. The composition of **2** consists of one less CO group than found in **1**, and the crystals incorporate a molecule of toluene in the crystalline lattice, as confirmed by the ^{1}H NMR spectrum and the crystal structure shown in the ORTEP diagram, Figure 3. The crystals melt with decomposition at 211−215 °C and do not yield a molecular ion in the mass spectrum.

The molecule has idealized C_2 symmetry; the C_2-axis is colinear with the C−O bond and takes Ce(1) into Ce(1_2) and the front left Cp′-ring into the back right Cp′. The two metallocene fragments are orientated such that the dihedral angle formed by the intersection of the planes defined by the Cp′(ring perpendicular)−Ce(1)−Cp′(ring perpendicular) and Cp′(ring perpendicular)−Ce(1_2)−Cp′(ring perpendicular) is 27°. The orientation of the individual cyclopentadienyl rings is staggered with a Cp′(ring perpendicular)−Ce−Cp′(ring perpendicular) angle of 135°. The averaged Ce−C distance is identical to the value found in the enediolates, **1-cis** and **1-trans**, but the Ce(1)−O(1) distance of 2.443(2) Å is much longer. The Ce(1)−C(35) distance is 2.554(4) Å identical to that found in $(C_5Me_5)_2CeCH(SiMe_3)_2$ where the Ce−C(alkyl) distance is 2.556(5) Å.[18] The Ce(1)−O(1) and Ce(1_2)−O(1) distances are equivalent by symmetry as are the Ce(1)−C(35) and Ce(1_2)−C(35) distances, which generates a planar formaldehyde dianion containing a five coordinate and therefore hypervalent carbon atom.[19a] This is an artifact that is most likely due to a superposition of two enantiomers of C_2-symmetry, **A** and **B** (Chart 1). A structure in which the formaldehyde dianion is planar is most unlikely because the two electrons added to the LUMO of neutral CH_2O requires mixing the π^* orbital with the empty σ^* orbital of the same symmetry, which localizes the negative charge on the carbon and oxygen atom as shown by **C** (Chart 1), generating a CH_2O fragment with a C−O single bond and a carbon atom that is essentially sp^3-hybridized.[19b] The observed C−O distance of 1.39(1) Å is close to that found in ethyleneglycol of 1.416(5) Å[19c] and consistent with this rationalization.

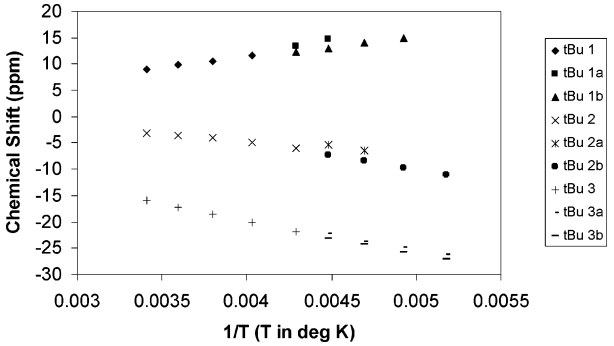

Figure 4. Chemical shift vs $1/T$ for $(Cp'_2Ce)_2(\mu\text{-}OCH_2)$ (**2**).

This bond model is also consistent with the geometry found for the CH_2O fragment in $(Cp_2ZrCl)_2(CH_2O)$ in which the Zr−O distances are nearly equal, 2.13(1) and 2.11(1) Å, but the Zr−C distances are not, 2.19(1) and 3.07(1) Å.[20a] A similar pattern is observed in two other compounds with bridging CH_2O groups, $(Cp_2Zr)_3(CH_2O)_3$[20b] and $\{(\eta^8\text{-}C_8H_8)Zr(O\text{-}(2,6\text{-}(Me_3C)_2C_6H_3)\}_2(CH_2O)$.[20c] The C−O distance in these three structures range from 1.31(1) to 1.43(1) Å, which is also consistent with the model illustrated by **C**.

The ^{1}H NMR spectrum at temperatures below −50 °C has a pattern of six Me_3C-resonances similar to that of the enediolate in this temperature range as shown by comparing Figure 2 with Figure 4. As the temperature is increased, the Me_3C-resonances pairwise merge into three equal area resonances whose chemical shifts are linear in $1/T$ up to 20 °C; heating to higher temperature results in an irreversible reaction, see later. A physical model that accounts for the low-temperature spectrum is similar to that advanced for **1**, *viz.*, the cyclopentadienyl rings are not freely rotating about their pseudo-C_5 axes at the lowest temperature, generating a molecule with C_2 symmetry. Warming increases the oscillatory motion of the Cp′-rings resulting in time averaged C_{2v} symmetry; because the vertical symmetry plane does not interconvert the CMe_3-groups on a given Cp′-ring, three CMe_3-resonances are observed. This model assumes that the enantiomers are interconverting rapidly throughout the temperature range.

As previously mentioned, **2** turns deep red purple on heating in a sealed capillary as it melts at 211−215 °C. Examination

(18) Heeres, H. J.; Meetsma, A.; Teuben, J. H.; Rogers, R. D. *Organometallics* **1989**, *8*, 2637.

(19) (a) Albright, T. A.; Burdett, J. K.; Whangbo, M. H. *Orbital Interactions in Chemistry*; Wiley: New York, 1985. (b) Levin, C. C. *J. Am. Chem. Soc.* **1975**, *97*, 5649. (c) Sutton, L. E. *Tables of Interatomic Distances and Configuration in Molecules and Ions. Supplement 1*; The Chemical Society: London, UK, 1965.

(20) (a) Gambarotta, S.; Floriani, C.; Chiesi-Villa, A.; Guastini, C. *J. Am. Chem. Soc.* **1983**, *105*, 1690. (b) Kropp, K.; Skibbe, V.; Erker, G.; Krüger, C. *J. Am. Chem. Soc.* **1985**, *105*, 3353. (c) Berno, P.; Floriani, C.; Chiesi-Villa A., Guastini, C. *J. Chem. Soc. Chem. Commun.* **1991**, 109.

Scheme 2. Postulated Reaction Pathways for Formation of **1-cis**

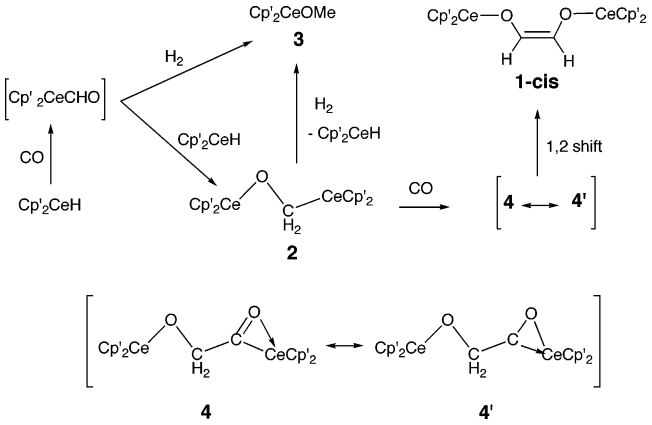

Chart 2. Left, Sawhorse Representations and Right, Newman Projections

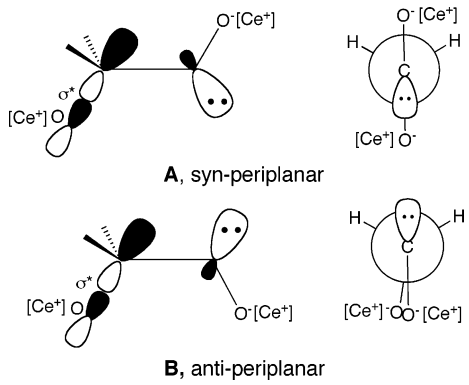

of the red purple melt by ^{1}H NMR spectroscopy in C_6D_6 shows resonances due to the metallacycle, Cp′[(Me$_3$C)$_2$C$_5$H$_2$C(Me)$_2$-CH$_2$]Ce[14] and a new pair of Me$_3$C-resonances in a 2:1 area ratio. The mass spectrum of **2** also shows fragment ions due to the metallacycle and metallacycle plus 32 amu, *i.e.*, Cp′$_2$CeOMe, **3**, which could arise from decomposition of **2** by transfer of a hydrogen atom from a ring Me$_3$C group to the oxomethylene group. This transformation may be observed directly by ^{1}H NMR spectroscopy. In C_6D_{12} solution, the 1:1:1 pattern of the Me$_3$C-resonances of **2** gradually disappear over 2 days at 20 °C and resonances identical to those observed from the melt decomposition appear. These experiments suggest that if an alternative source of hydrogen were present, **2** would yield **3**.

This hypothesis is true, because addition of dihydrogen to **2** dissolved in C_6D_6 in a NMR tube generates resonances due to Cp′$_2$CeH and the two new Me$_3$C-resonances mentioned previously that were suggested to be due to **3**, a conjecture shown to be correct by independent synthesis. Addition of a CO:H$_2$ mixture (1:10) to Cp′$_2$CeH in C_6D_6 in a NMR tube generates resonances due to Cp′$_2$CeH and the new set of resonances due to **3**. Successive addition of the CO:H$_2$ mixture results in disappearance of the resonances due to Cp′$_2$CeH and cleanly generates a spectrum that contains only the resonances due to **3**. On a synthetic scale, addition of a CO:H$_2$ mixture to Cp′$_2$CeH in pentane gives a red solution, from which the methoxide, **3**, may be isolated, Scheme 1. Repeating the reaction of **2** with CH$_4$ rather than H$_2$ results in formation of **3** and the metallacycle; methane cannot be used as a hydrogen source or reactant in the reactions shown in Scheme 1. The product of reaction between Cp′$_2$CeH and syngas is Cp′$_2$CeOMe. This transformation is not catalytic because H$_2$ does not cleave the Ce−O bond, but the stoichiometric reaction is a model for the initiation of the catalytic hydrogenation of carbon monoxide.

Isotopic Labeling and Mechanism. The mechanisms of the net reactions illustrated in Scheme 1 are not easily studied. The original plan was to use deuterium labeled Cp′-groups in crossover experiments, however the labeled and unlabeled Cp′-groups exchange and therefore analysis by mass spectroscopy is inappropriate.[21] Accordingly, an alternative and less quantitative strategy was devised. Compound **1**, prepared from either $^{13}C^{16}O$ or $^{12}C^{18}O$, is used to determine the molecularity of the isomerization reaction of **1-cis** to **1-trans**. The $^{12}C^{18}O$ labeled carbon monoxide is preferred for mass spectroscopic analysis because the mass changes by 2 amu relative to unlabeled carbon monoxide. The initial experiment designed to establish the extent of enrichment, is exposure of Cp′$_2$CeH to $^{12}C^{18}O$ in pentane to give **2-^{18}O** that, when exposed to H$_2$ gives **3-^{18}O**. Analysis by mass spectrometry showed that the $^{12}C^{18}O$ was at least 99% enriched. Oxygen-18 labeled **1-cis(^{18}O$_2$)** is prepared by exposing Cp′$_2$CeH to $^{12}C^{18}O$ in toluene, evaporating the solvent and analyzing the solid by mass spectroscopy. Addition of $^{13}C^{16}O$ to Cp′$_2$CeH in C_6D_6 in an NMR tube gives **1-cis** in which the olefinic carbon atoms in the enediolate bridge are labeled with ^{13}C as shown by the appearance of a doublet in the ^{1}H NMR spectrum at $\delta = 39$, $^1J_{CH} = 180$ Hz. Removal of the excess $^{13}C^{16}O$, replacing the gas by $^{12}C^{16}O$, and heating at 60 °C for 2 months results in approximately 90% conversion of **1-cis-(^{13}C$_2$)** to **1-trans(^{13}C$_2$)** with $\delta = 35$, $^1J_{CH} = 190$ Hz. Addition of Me$_3$SiN$_3$ followed by hydrolysis and analysis by GCMS showed only a cis and trans mixture of 1,2-(Me$_3$SiO)$_2$^{13}C$_2$H$_2$. Repeating the experiment with **1-cis(^{18}O$_2$)** in presence of $^{12}C^{16}O$ showed no ^{16}O-label incorporated into *cis*- and *trans*-1,2-(Me$_3$Si^{18}O)$_2$C$_2$H$_2$. Thus, the isomerization is intramolecular.

The generally accepted mechanism for formation of enediolate complexes from a metal hydride and carbon monoxide, when applied to Cp′$_2$CeH, is illustrated in Scheme 2.[5,11] Coordination of CO to Cp′$_2$CeH is followed by hydrogen migration, generating the formyl Cp′$_2$CeCHO, which is trapped by Cp′$_2$CeH to give **2**, an isolated compound, or by H$_2$ to give **3**, also an isolated compound. In absence of H$_2$, the oxomethylene **2** reacts with excess CO generating **4**, symbolized by the two resonance structures **4** and **4′**. A 1,2-hydrogen shift, which is either a proton transfer or an insertion of the carbenoid into the C−H bond, yields the *cis*-enediolate, **1-cis**, an isolated compound.

A new aspect described in this article is the irreversible isomerization of **1-cis** to **1-trans**, which generates the obvious question of why the cis isomer is the kinetic isomer and the trans isomer is the thermodynamic one.[22] A rationalization for a lower barrier to form the cis isomer, relative to the trans isomer, is provided by the Newman projections viewed down the C−C bond of resonance structure **4′** (Chart 2). In **A**, the orientation of the carbenoid lone pair is syn-periplanar, whereas

(21) Compounds **1** and **3** give molecular ions in their mass spectra. The Me$_3$C groups are readily deuterated[14] to give {[(CD$_3$)$_3$C]$_3$C$_5$H$_2$}$_2$CeD, (Cp-d$_{27}$)$_2$-CeD, which reacts with CO in pentane to give **2-d$_{110}$**. Mixing **2-d$_0$** and **2-d$_{110}$** in toluene followed by addition of CO, isolation and analysis by mass spectroscopy shows molecular ions due to **1-d$_0$**, **1-d$_{28}$**, **1-d$_{56}$**, **1-d$_{84}$**, and **1-d$_{110}$**. A similar result is obtained when **2-d$_0$** and **2-d$_{110}$** were stirred in toluene for 30 minutes followed by analysis of the solid material by mass spectroscopy. In both experiments, the Cp′-rings exchange in solution and/or in the mass spectrometer.

(22) Berson, J. A. *Angew. Chem. Int. Ed.* **2006**, *45*, 4724.

Chart 3

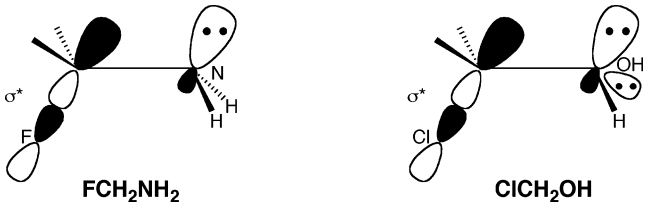

in **B**, it is anti-periplanar, relative to the CO bond of the OC-(H_2) unit in the $-OCH_2CO^-$ fragment. If one of these orientations is lower in energy then the 1,2-hydrogen shift will occur in the rotamer of lower energy.

Calculations on model systems such as FCH_2NH_2[23a] and $ClCH_2OH$[23b] show that the anti-periplanar orientation of the halide ligand relative to the lone pair of electrons on nitrogen or oxygen is about 5 kcal mol^{-1} lower in energy than in the syn-periplanar orientation (Chart 3). The anti-periplanar orientation allows a better overlap of the high-lying lone pair with the empty σ^* orbital of the adjacent polar bond (C−F, C−Cl).[23c]

Extrapolating these results to the more complex organometallic compounds described here, traces the cis stereochemistry of the enediolate to a stereoelectronic effect in the carbenoid fragment that sets the stereochemistry for the 1,2-hydrogen shift. The lone pair of electrons on carbon is stabilized by an interaction with the σ^*_{CO} orbital in the anti-periplanar orientation. This is supported by a DFT calculation on the model compound $(MeO)CH_2C(OMe)$, which shows that the conformation with the anti-periplanar orientation of the carbenoid lone pair is 1.5 kcal mol^{-1} lower in energy than with the syn-periplanar orientation. In this model, steric effects are assigned only a modest role, because, in either rotamer, the bulky Cp'_2Ce metallocenes have an anti orientation relative to the CC bond, in the crystal structures of **1-cis** and **1-trans**.

The final product is **1-trans**, formed by an intramolecular rearrangement of **1-cis,** which shows that the trans enediolate is more thermodynamically stable than the cis-enediolate and the physical process for the isomerization is, presumably, rotation about the carbon−carbon double bond. Calculations of the rotational energy barrier in molecules as complex as **1-cis** and **1-trans** are impossible; the calculation is even difficult in molecules as simple as ethylene.[24] Furthermore, the calculations of **1-trans** and **1-cis** did not converge, and the complexes appear to be very floppy. It is straightforward, however, to calculate the heats of hydrogenation of olefins ($CH_2{=}CH_{2(g)} + H_{2(g)} \rightarrow C_2H_{6(g)}$), which is a measure of their π-bond energies. The calculated heat of hydrogenation (kcal mol^{-1}) decreases in the order: $CH_2{=}CH_2$ (44), FHC═CHF (40),[25] (MeO)HC═CH-(OMe) (34), $(H_3SiO)HC{=}CH(OSiH_3)$ (33), and (KO)HC═CH-(OK) (20). This order is associated with the electron delocalization from the lone pairs on the heteroatoms into the π^*_{CC} orbital, which increases in the order F < OMe < $OSiH_3$ < OK, and therefore weakening the carbon−carbon double bond.[26a] If the π-bond energy is proportional to the rotation barrier in 1,2-disubstituted ethylenes, then the rotation barrier for isomerization of **1-cis** to **1-trans** is not unreasonably high. Calculating the relative energies of **1-cis** and **1-trans** also is impossible. However, calculations on several 1,2-disubstituted ethylenes of the type $C_2X_2H_2$ (X = F, OMe, $OSiH_3$) show that the cis and trans isomers are very close in energy,[26b] which if true for **1-cis** and **1-trans**, supports the notion that formation of the cis-isomer is under kinetic control.

Computational Studies. The reaction mechanism for the reaction of Cp'_2CeH and CO with H_2 is analyzed by DFT-(B3PW91) calculations. No calculations were carried out for the reaction of Cp'_2CeH and CO in absence H_2 because the complexes contain two cerium fragments that are too large to be accurately treated.

In the calculations, Cp'_2CeH is modeled by Cp_2CeH, which changes the steric effects of the metallocene fragment.[27] The CO and H_2 reactants are small molecules and steric effects are likely to play only a minor role in the relative activation energies. This approach was used successfully in a number of previous studies.[14,28] Many computational studies of reactivity are discussed on the basis of changes in free energy (ΔG) and not in energy (ΔE), because it is not reasonable to ignore the entropic factor in a reaction where the number of molecules is not constant. However, using entropic values calculated in the gas phase for reactions that occur in solution is controversial.[29] For these reasons, we report ΔG and ΔE values. The activation energy ($\Delta G^{\ddagger}$) and energy barrier ($\Delta E^{\ddagger}$) are similar for all of the individual steps in the reaction described here, the only difference is the loss of translation entropy when two molecules merge into one. The conclusions derived by consideration of either ΔG or ΔE are similar and only ΔG values are used in the text; the energy values are given in the Supporting Information.

Reaction of Cp_2CeH with CO: Formation of a Formyl Complex. The structures of all extrema (minima and transition states) are shown in Figure 5, and the free energy profile (ΔG) is shown in Figure 6. The reaction begins by coordination of CO to Cp_2CeH, **5**. Even though the H−Ce−C(O) angle of 120° is large, the addition of CO does not perturb the Cp−Ce−Cp angle; it is 136° in Cp_2CeH and 135° in $Cp_2CeH(CO)$. The small binding energy of CO in **5** of 9.8 kcal mol^{-1}, is due to the lack of back-donation from the metal and the interaction is essentially an electrostatic one in which little charge transfer occurs. The corresponding free energy change for CO coordination is

(23) (a) Irwin, J. J.; Ha, T.-K.; Dunitz, J. D. *Helv. Chim. Acta* **1990**, *73*, 1805. (b) Omoto, K.; Marusaki, K.; Hirao, H.; Himade, M.; Fujimoto, H. *J. Phys. Chem. A* **2000**, *104*, 6499. (c) Hoffmann, R.; Imamura, H.; Hehre, W. J. *J. Am. Chem. Soc.* **1968**, *90* 1499.

(24) Schmidt, M. W.; Truong, P. N.; Gordon, M. S. *J. Am. Chem. Soc.* **1987**, *109*, 5217. Wang, Y.; Poirier, R. A. *Can. J. Chem.* **1998**, *76*, 477.

(25) The decrease in the π-bond energy and of the rotational barriers around the CC bond with increasing number of fluorines has been the subject of high-level calculations.[24]

(26) (a) The antibonding character of the olefinic carbon atoms in the HOMO-1 orbital in the six π-electron systems of the cis- or trans-1,2-disubstituted olefins increases with the electron donating ability of the π bonded lone pair. (b) Epiotis, N, D. *J. Am. Chem. Soc.* **1973**, *95*, 3087. Epiotis, N. D.; Yates, R. L. *J. Am. Chem. Soc.* **1976**, *98*, 461.

(27) Modeling of Cp′ by Cp also changes the Cp(ring centroid)−Ce−Cp(ring centroid) angle, which in turn effects the dipole moment of the Cp_2CeX fragment; steric and electronic effects are not independent, but the calculated trends for the reactions are likely to be well represented.

(28) (a) Maron, L.; Eisenstein, O. *J. Am. Chem. Soc.* **2001**, *123*, 1036. (b) Maron, L.; Perrin, L.; Eisenstein, O. *J. Chem. Soc. Dalton Trans.* **2002**, 534. (c) Perrin, L.; Maron, L.; Eisenstein, O. *Dalton. Trans.* **2003**, 4313. (d) Perrin, L.; Maron, L.; Eisenstein, O. *New J. Chem.* **2004**, *28*, 1255. (e) Niu, S. Q; Hall, M. B. *Chem. Rev.* **2000**, *100*, 353.

(29) Cooper, J.; Ziegler, T. *Inorg. Chem.* **2002**, *41*, 6614. Sakaki, S.; Takayama, T.; Sumimoto, M. Sugimoto, M. *J. Am. Chem. Soc.* **2004**, *126*, 3332. Rotzinger, F. P. *Chem. Rev.* **2005**, *105*, 2003. Leung, B. O.; Reidl, D. L.; Armstrong, D. A.; Rauk, A. *J. Phys. Chem. A* **2004**, *108*, 2720. Ardura, D.; Lopez, R.; Sordo, T. L. *J. Phys. Chem. B* **2005**, *109*, 23618. Raynaud, C.; Daudey, J.-P.; Jolibois, F.; Maron, L. *J. Phys. Chem. A* **2006**, *110*, 101.

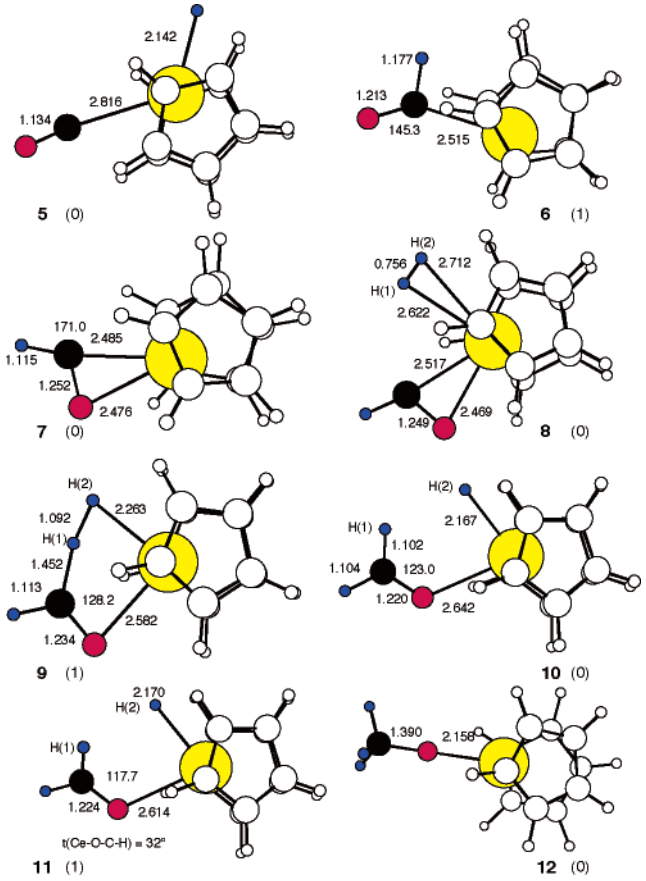

Figure 5. Optimized DFT(B3PW91) structures for the reaction $Cp_2CeH + CO + H_2$ to form $Cp_2Ce(OMe)$, distances are in Å and bond angles and torsional angle (*t*) are in degrees. Minima and transition states are indicated by the number, in parentheses, of imaginary frequencies, 0 and 1 respectively.

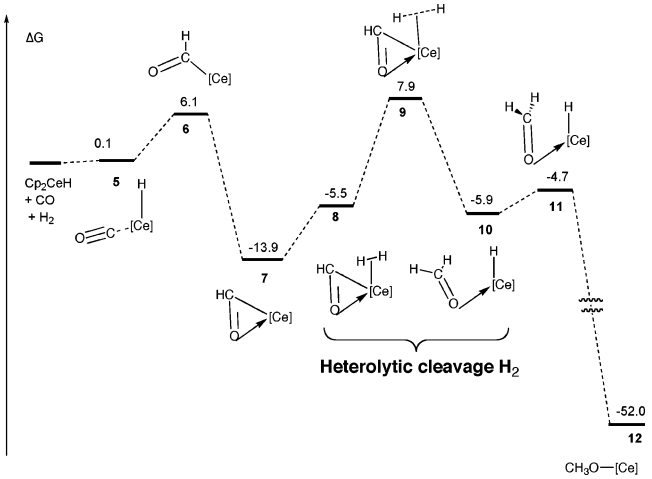

Figure 6. Free energy profile (kcal mol^{-1}) for the reaction $Cp_2CeH + CO + H_2$ to form $Cp_2Ce(OMe)$.

essentially zero, and therefore, coordinated and free CO are in equilibrium.[30] A transition state **6**, for insertion of CO into the Ce−H bond has been located, with a low activation energy of 6.0 kcal mol^{-1} above **5**. The transition state **6** is an η^1-formyl complex with a Ce−C distance of 2.52 Å, a fully formed C−H bond of 1.18 Å and a rather large Ce−C−O angle of 145°. The transition state **6** connects to an η^2-formyl complex, **7**, which is 13.9 kcal mol^{-1} below the separated reactants, Cp_2-CeH and CO. In **7**, the Ce−C and Ce−O distances are equal (2.48 Å), the C−O distance is 1.25 Å and the Ce−C−H angle to 171°. A similar geometrical pattern was calculated for the η^2-formyl complex resulting from the insertion of CO into the Sc−H bond of Cl_2Sc−H.[31] A similar structure is found in early transition metal acyl complexes which show essentially equal M−C and M−O distances, an acute M−C−O angle of about 75° and an open M−C−R angle. For example, the M−C−C(methyl) angle is 163° in $(C_5Me_5)_2Zr(\eta^2$-COMe)CO[32a] and 169° in $(C_5Me_5)_2Th(\eta^2$-CO−CH_2−$CMe_3)Cl$.[32b] As will be shown later, the open M−C−H angle and therefore the orientation of the frontier orbitals plays a key role in the reactivity of the formyl group. The formation of the η^2-formyl complex is exoergic and proceeds with a low activation energy.

The formation of the formyl complex is the primary event and different reaction pathways are followed depending on the presence or absence of H_2.

Reaction of the η^2-Formyl Complex with H_2. Dihydrogen interacts with the η^2-formyl complex **7** to form a H_2 adduct, **8**. The H_2 binds weakly (<1 kcal mol^{-1}) and **8** is therefore 8.4 kcal mol^{-1} above the separated reactants, **7** and H_2, due to the entropy change. The dihydrogen-formyl complex **8** is transformed into a cerium hydride coordinated to a formaldehyde molecule by transition state **9**. At the transition state **9**, the H−H bond is cleaved in a process reminiscent of a proton-transfer transition state because the C−H(1)−H(2) angle is nearly linear (167°). The transfer of H(1) to the formyl carbon lengthens the Ce−C bond and opens slightly the Ce−O−C angle from 73° to 82°. At **9**, all bonds are partially made or broken in a synchronous way that results in cleavage of the H−H and the Ce−C bonds and in formation of the C−H and Ce−H bonds; the H(1)−H(2) and Ce−C distances lengthen to 1.09 and 2.69 Å, respectively, and the new C−H(1) and Ce−H(2) bonds are 1.45 and 2.26 Å, respectively. The activation energy for the proton transfer is 13.4 kcal mol^{-1} above **8**; therefore, the transition state **9** is only 7.9 kcal mol^{-1} above separated reactants Cp_2CeH, CO, and H_2. The proton transfer gives the formaldehyde complex $Cp_2CeH(O{=}CH_2)$, **10**. In **10**, the formaldehyde is coordinated to the Cp_2CeH fragment by an oxygen lone pair, the C−O−Ce angle of 123° is typical for aldehydes and ketones coordinated to Lewis acids.[33] The formaldehyde and the Ce−H bond are coplanar so that the π^* orbital of the formaldehyde does not interact with the hydride. The formyl-dihydrogen complex, **8** and the cerium-hydride formaldehyde complex, **10**, have essentially the same free energy and they are related by a transition state with a low activation energy that is a proton transfer. The transformation of the formaldehyde-hydride, **10**, via the transition state **11** into the methoxide complex, **12**, is exoergic by 46.1 kcal mol^{-1} and proceeds with a negligible activation energy. The transition state **11** is therefore strongly reactantlike. A rotation of the formaldehyde by 32° out of the H(2)−Ce−O plane is the only noticeable change in geometry between **10** and **11**, Chart 4. Due to the strong exothermicity

(30) Maron, L.; Perrin, L. Eisenstein, O.; Andersen, R. A. *J. Am. Chem. Soc.* **2002**, *124*, 5614.
(31) Rappé, A. K. *J. Am. Chem. Soc.* **1987**, *109*, 5605.
(32) (a) Guo, Z.; Swenson, D. C.; Guram, A. S.; Jordan, R. F. *Organometallics* **1994**, *13*, 766. (b) Fagan, P. J.; Manriquez, J. M.; Marks, T. J.; Day, V. W.; Vollmer, S. H.; Secaur Day, C. *J. Am. Chem. Soc.* **1980**, *102*, 5393.
(33) Branchadell, V.; Oliva, A. *J. Am. Chem. Soc.* **1991**, *113*, 4132. Branchadell, V.; Oliva, A. *J. Am. Chem. Soc.* **1992**, *114*, 4357.

Chart 4. Views of **10** and **11** down the O−Ce Bond

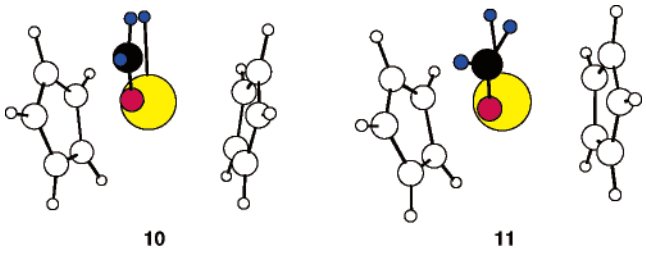

10 **11**

of this step, a small rotation of the formaldehyde and thus a small overlap between the empty π^* orbital of the formaldehyde and the hydride is sufficient to render the hydride nucleophilic so that it adds to the formaldehyde activated by coordination to the electropositive Cp_2Ce fragment.[34]

A number of computational studies on the structure and formation of formyl complexes due to migratory insertion of CO have been reviewed.[28e,35] The preference for an η^2-coordination of the CHO fragment for early transition metal and for η^1 coordination for late transition metal complexes is established by EHT calculations.[36a] The mechanism for CO migratory insertion in $Cp_2Zr(CH_3)_2$ was studied with DFT[36b] and with ab initio dynamic methods[36c] with special focus on the inside−outside orientation for insertion. The mechanism for transition metal promoted reductive CO coupling with zirconocene[36d] and with actinocene[36e] has been analyzed by MO theory using EHT calculations. The origin of the energy barrier for migratory insertion of CO into the late transition metal M−R bond was discussed using a similar methodology[37a] and the influence of R on the kinetics and thermodynamics of the migratory insertion has been analyzed with self-consistent semiempirical methods.[37b] Early ab initio studies show that the formation of the formyl complex in late transition metal complexes is kinetically difficult and thermodynamically unfavorable[37c] and that the acetyl fragment is lower in energy than the formyl fragment.[37d] In the GVB analysis of the insertion of CO in Cl_2ScH, the geometries of the transition state and minimum found for the insertion of CO in the Sc−H bond of Cl_2ScH are similar to that of **6** and **7**.[31] The notable features are the similar M−C and M−O distances, the acute M−C−O and open M−C−H angles (171° for Ce and 176° for Sc). This leads to a H−C−O angle of 114° for Ce and 118° for Sc. As mentioned earlier, the experimental structures of acetyl complexes display similar features. The unusual geometry at carbon, which is far from sp^2 hybridization, is a distinctive feature. The GVB analysis shows that the Sc−C bond in the Sc−CO three member ring is not along the Sc−C axis; the two electrons in the bond are mostly localized on the carbon and orientated as schematically shown as **a** in Chart 5. Remarkably, the lone pair on carbon of an isolated $HCO^{(-)}$ anion has a similar orientation. Although no GVB analysis can be carried out on $Cp_2Ce(\eta^2$-CHO), the NBO analysis and reactivity are consistent with a similar bonding pattern.

Chart 5

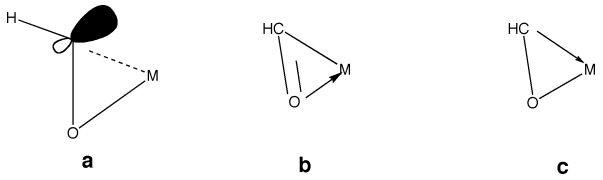

The NBO charge on the oxygen atom is −0.72 and that on the carbon atom is −0.2 (**7** in Figure 7); the total negative charge on the ligand is close to unity. The free formyl anion is a 12-electron molecule that is strongly bent at carbon as shown by a qualitative MO analysis,[38a] experiment (109 ± 2°),[38b] and CCSD(T) calculations (109.8°).[38c] The formyl anion interacts with Ce mostly by way of the oxygen atom, which means that the lone pair is essentially localized on the carbon in the Ce−C−O plane. Thus, the fragment has the geometry of a carbenoid fragment (oxycarbenoid), with a high electron density on the carbon atom in the Ce−C−O plane and a low lying empty orbital perpendicular to that plane.[38d] This agrees with the postulate that the MCHO is "carbene-like" in the metal acyl complexes.[38e] Because the lone pair on carbon does not point directly toward the metal atom (Chart 5, **a**) and because the charge carried by the carbon atom is rather small, the bond to cerium is rather weak. The CHO orientation requires little reorganization for accepting the proton in the proton-transfer step in transition state **9**.

The valence bond structures of the acyl of formyl metal complexes can be written as **b** or **c** in Chart 5 (this is analogous to the **4** and **4′** resonances structures in Scheme 2). The negative density on C as well as on O indicated by the NBO analysis supports the dominant influence of valence bond structure **c**. In the case of $Cl_2Sc(\eta^2$-CHO), however, Rappé considers that the dominant structure is **b**.[31] The dominance of the valence bond structure **c** is consistent with the nucleophilic reactivity displayed by the formyl complex (see later).

The NBO charges for the extrema for the insertion of CO into the Ce−H bond are given in Figure 7. The hydrogen atom is strongly hydridic in Cp_2CeH (−0.69), essentially neutral in the transition state **6** and carries a positive charge (+0.16) in the η^2-formyl complex **7**. The density on C(O) in **6** is high (−0.26), decreases slightly in **7**, whereas the negative charge on the oxygen atom increases from **6** (−0.54) to **7** (−0.72). The positive charge on Ce marginally increases on going from the cerium hydride complex to the cerium formyl, **7**, to maintain electroneutrality, because the negative charge on the oxygen atom increases. At the transition state **9**, H(2) has a large negative charge (−0.42). The hydrogen atom that is transferred, H(1), is essentially neutral as is the carbon atom to which it is transferred. The oxygen atom is slightly less negatively charged. Thus at **9**, the charge distribution is consistent with the

(34) Corma, A.; Garcia, H. *Chem. Rev.* **2003**, *103*, 4307.
(35) Torrent, M.; Sola, M.; Frenking, G. *Chem. Rev.* **2000**, *100*, 439.
(36) (a) Hofmann, P.; Stauffert, P.; Tatsumi, K.; Nakamura, A.; Hoffmann, R. *Organometallics* **1985**, *4*, 404. Tatsumi, K.; Nakamura, A.; Hofmann, P.; Stauffert, P.; Hoffmann, R. *J. Am. Chem. Soc.* **1985**, *107*, 4440. (b) De Angelis, F; Sgamellotti, A.; Re, N. *Organometallics* **2000**, *19*, 4904. (c) De Angelis, F.; Sgamellotti, A.; Re, N. *J. C. S. Dalton Trans.* **2001**, 1023. Fantacci, S.; De Angelis, F.; Sgamellotti A.; Re, N. *Organometallics* **2001**, *20*, 4031. De Angelis, F.; Fantacci, S.; Sgamellotti A. *Chem. Coord. Rev.* **2006**, *250*, 1497. (d) Hofmann, P.; Frede, M.; Stauffert, P.; Lasser, W.; Thewalt, U. *Angew. Chem., Int. Ed.* **1985**, *24*, 712. Hofmann, P.; Stauffert, P.; Frede, M.; Tatsumi, K. *Chem. Ber.* **1989**, *122*, 1559. (e) Tatsumi, K.; Nakamura, A.; Hofmann, P.; Hoffmann, R.; Moloy, K. G.; Marks, T. J. *J. Am. Chem. Soc.* **1986**, *108*, 4467.
(37) (a) Berke, H.; Hoffmann, R. *J. Am. Chem. Soc.* **1978**, *100*, 7724. (b) Axe, F. U.; Marynick, D. S. *J. Am. Chem. Soc.* **1988**, *110*, 3728. (c) Nakamura, S.; Dedieu, A. *Chem. Phys.* Lett. **1984**, *111*, 243. Dedieu, A.; Sakaki, S.; Strich, A.; Siegbahn, P. E. M. *Chem. Phys. Lett.* **1987**, *133*, 317. (d) Dedieu, A.; Nakamura, S. *J. Organomet. Chem.* **1984**, *260*, C63.
(38) (a) Gimarc, B. M. *J. Am. Chem. Soc.* **1971**, *93*, 815. (b) Murray, K. K.; Miller, T. M.; Leopold, D. G.; Lineberger, W. C. *J. Chem. Phys.* **1986**, *84*, 2520. (c) van Mourik, T.; Dunning, T. H.; Peterson K. A. *J. Phys. Chem. A* **2000**, *104*, 2287. (d) Bourissou, D.; Guerret, O.; Gabbaï, F. P.; Bertrand, G. *Chem. Rev.* **2000**, *100*, 39. (e) Moloy, K. G.; Fagan, P. J.; Manriquez, J. M.; Marks, T. J. *J. Am. Chem. Soc.* **1986**, *108*, 56.

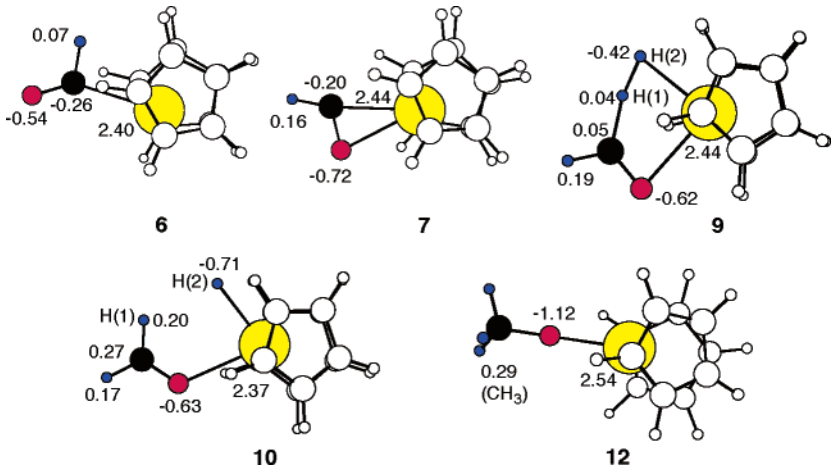

Figure 7. NBO charges for selected extrema in the pathway shown in Figures 5 and 6.

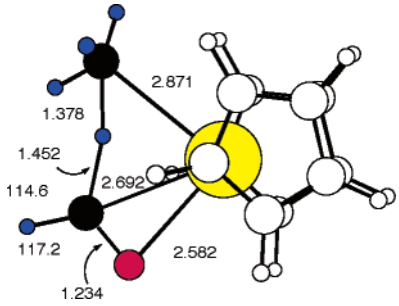

Figure 8. Transition state for $Cp_2Ce(\eta^2\text{-CHO}) + CH_4 \rightarrow Cp_2Ce(OCH_2)(CH_3)$.

heterolytic cleavage of dihydrogen. In the hydride-formaldehyde complex, **10**, the strong positive charge on C (+0.27) is characteristic of carbonyl groups activated by a Lewis acid. The strong negative charge on H(2) (−0.71) indicates its hydridic nature. In the methoxy complex, **12**, the charge on the oxygen is very large (−1.12) and the methyl group is positively charged (+0.29).

Heterolytic activation of dihydrogen generally is invoked when the removal of two electrons from the metal center is not energetically possible. Heterolytic cleavage of dihydrogen is well-known where dipolar dihydrogen adds to a M−X bond where X is more electronegative than M and is a key feature of the selective hydrogenation of polar bonds in the Noyori ruthenium catalyst.[39] In the present case, the carbon atom of the η^2-acyl accumulates electron density while the cerium atom carries a positive charge. The electron density on the carbon is located in the Ce−C−O plane and the dihydrogen must be coplanar with the Ce(η^2-CHO) bond in the transition state in order to optimize its overlap with Ce and the carbon atom of the formyl group. This reaction is therefore related to the addition of H_2 to Cp_2M-CH_3, where M is a lanthanide, to form an alkane and a lanthanide−hydride complex.[28b,40]

Table 1. Activation Energies (kcal mol^{-1}) for the Reaction [M]−R + H−R′ (R′ = H, CH_3) → [M]−R′ + R−H

[M]–R	data	H–H	H–CH_3
Cp_2Sc-H[41b,d]	$\Delta E^{\ddagger}$	2.2	16.8
Cp_2Sc-Me[41b,d]	$\Delta E^{\ddagger}$	6.0	16.8
[Si−O]Zt−H[41c]	$\Delta H^{\ddagger}$	4.4	20.6
[Si−O]Zr−CH_3[41c]	$\Delta H^{\ddagger}$	NA	25.5
Cp_2CeH	$\Delta G^{\ddagger}$	9.5	25.0
Cp_2Ce-CH_3	$\Delta G^{\ddagger}$	12.9	28.0
Cp_2Ce-(η^2-CHO)	$\Delta G^{\ddagger}$	21.9	38.9

Reaction of $Cp_2Ce(\eta^2\text{-CHO})$ with CH_4. The transition state for the reaction of the formyl complex with CH_4 to give a formaldehyde-methyl cerium complex was located 25 kcal mol^{-1} above the separated reactants Cp_2CeH, CO, and CH_4. The activation energy for the proton-transfer step is thus 39 kcal mol^{-1} relative to separated formyl complex and CH_4 and the reaction will not occur, as observed experimentally. The transition state, shown in Figure 8, has the geometry expected for a proton transfer from methane to the formyl group. The proton approaches the formyl group with a near-linear C···H···C angle as in the transition state **9** for H_2 activation. A linear transition state has been suggested based on primary isotope effects[41a] and on computational studies on related systems.[28a−c,39b,41b−f]

The activation energy for the reaction of CH_4 with the Ce-formyl group is 17 kcal mol^{-1} higher than for the reaction of H_2. This difference is not unique to the formyl complex just described, because computational studies show that replacing H_2 by CH_4 increases the activation energy by 15−18 kcal mol^{-1} in sigma-bond metathesis reactions of hydride or methyl complexes of various d^0 metals (Sc, Zr, Ce) (Table 1). The sigma-bond metathesis reaction of M−R + H_2 or H−CH_3 is a proton-transfer reaction, and therefore, the barrier is controlled by the acidity of the proton donor. The change in gas-phase enthalpy for the reaction of $CH_4(g) \rightarrow CH_3^-(g) + H^+(g)$ is 417 kcal mol^{-1} and that for $H_2(g) \rightarrow H^+(g) + H^-(g)$ is 400 kcal mol^{-1}.[42] The experimental result that methane is a poorer proton

(39) (a) Brothers, P. *Prog. Inorg. Chem.* **1981**, *28*, 1. Clapham, S. E.; Hadzovic, A.; Morris, R. H. *Coord. Chem. Rev.* **2004**, *248*, 2201. Noyori, R.; Hashiguchi S. *Acc. Chem. Res.* **1997**, *30*, 97. Abdur-Rashid, K.; Clapham, S. E.; Hadzovic, A.; Harvey, J. N.; Lough, A.; J.; Morris, R. H. *J. Am. Chem. Soc.* **2002**, *124*, 15104. Lee, D.-H.; Patel, B. P.; Crabtree, R. H.; Clot, E.; Eisenstein, O. *Chem. Commun.* **1999**, 297. Gruet, K.; Clot, E.; Eisenstein, O.; Lee, D. H.; Patel, B.; Macchioni, A.; Crabtree, R. H. *New J. Chem.* **2003**. *27*, 80. Kubas, G. J. *Adv. Inorg. Chem.* **2004**, *56*, 127. (b) Chan, B.; Radom, L. *J. Am. Chem. Soc.* **2005**, *127*, 2443.
(40) Perrin, L.; Maron, L.; Eisenstein, O. *Organometallic C-H Bond Activation*; Goldman, A.; Goldberg, K. Eds; ACS Book Series 885; American Chemical Society: Washington D.C., 2004; p 116.
(41) (a) Sadow, A.; Tilley, T. D. *J. Am. Chem. Soc.* **2003**, *125*, 7971. (b) Ziegler, T.; Folga, E; Berces, A. *J. Am. Chem. Soc.* **1993**, *115*, 636. (c) Copéret, C; Grouiller, A.; Basset, J.-M.; Chermette, H. *Chem. Phys. Chem.* **2003**, *4*, 608. (d) Sherer, E. C.; Cramer, C. J. *Organometallics* **2003**, *22*, 1682. (e) Woodrum, N. L.; Cramer, C. J. *Organometallics* **2006**, *25*, 68. (f) Barros, N.; Eisenstein, O.; Maron, L. *Dalton Trans.* **2006**, 3052.
(42) Bartmess, J. E.; McIver, R. T. *Gas Phase Ion Chemistry*; Bowers, M. T., Ed.; Academic Press: New York, 1979; Vol 2, p 87.

donor than dihydrogen by 17 kcal mol^{-1} supports the interpretation of the computational results that sigma-bond metathesis transition states resemble proton-transfer transition states, i.e., they are proton-transfer reactions. A corollary is the expectation that methane activation will always be more difficult than dihydrogen activation by about 15−18 kcal-mol^{-1} when oxidative addition does not occur. Furthermore, increasing the acidity of the alkane by an electronegative substituent, such as F, lowers the activation energy for proton transfer.[14b] The relative rate of reaction of R−H with Cp^*_2Sc-R' (R = R′ = H >> R = H, R′ = alkyl > R = sp^3 C−H, R′ = alkyl) is suggested to be due to the decreases in the s-character of the reacting bond,[43a] which is consistent with the proposition advanced above because the acidity of R−H is related to the s-character in the C−H bond.[43b] The difference in reactivity of Cp_2CeX (X = H, alkyl, formyl) is related to the electron affinity and electronegativity of X. All of the ligands bonded to a lanthanide carry a negative charge, because the total charge on the metal is about +2.4 for cerium in these metallocenes. The total charge on X is essentially constant because the charge on Cp does not change among these various complexes. For X = H and CH_3, the negative charge is concentrated on these atoms or groups whereas, in the formyl, the negative charge is largely localized on oxygen (−0.7) and less (−0.2) on carbon. Because the carbon atom carries a smaller negative charge, the nucleophile character is less than when X = H or CH_3, which results in a higher activation energy for a proton-transfer reaction. This explanation can be used to rationalize why the metallacycle, $Cp'[(Me_3C)_2C_5H_2C(CH_3)_2CH_2]$-Ce, reacts with CH_4 or more acidic hydrocarbons such as benzene; the metallated carbon of the cyclopentadienyl ligand is likely to a carry a negative charge similar to that in a methyl group.[14] It is worth noting that the kinetic and thermodynamic conditions for a Ce−X bond to activate a C−H bond are very stringent. In order for the C−H activation to occur, X must carry a large negative charge to favor the proton transfer and the thermodynamics must be favorable. An X atom more electronegative than carbon carries a large negative charge but the thermodynamics of the exchange reaction $Cp_2CeX + H-CH_3 \rightarrow Cp_2CeCH_3 + HX$ are endothermic because of the strong Ce−X bond. In order to achieve a metathesis of X for CH_3 in methane, at a d^0 metal center, X must have an electronegativity comparable to that of carbon, which leads to the prediction that only degenerate or nearly degenerate hydrocarbyl exchange has a low-energy barrier. This leads to the generalization that only a metal-alkyl bond is able to activate an alkane C−H bond, i.e., degenerate metathesis.

Epilog. Several fundamental concepts emerge from the experimental and computational study described here. The experimental studies show that the net reaction of Cp'_2CeH with CO and H_2 is Cp'_2CeOMe, (**3**), i.e., hydrogenation of CO. When H_2 is absent, the dimetal products **1** or **2** are formed; **1** is formed from **2** when CO is added and **3** is formed from **2** when H_2 is added. Thus, **2** is a key compound in unraveling the mechanism of the net reaction, because insertion of CO results in a hypothetical $-OC(H_2)\ddot{C}O^-$ fragment in which the lone pair of electrons on the carbenoid carbon atom is antiperiplanar relative to the $O-C(H_2)$ bond. This conformation determines the stereochemical outcome of a 1,2-hydrogen shift resulting in formation of **1-cis**, the kinetic product. The kinetic product irreversibly isomerizes to **1-trans**, the thermodynamic product.

The computational results show that the net reaction of Cp_2CeH with CO and H_2 to form Cp_2CeOMe is exoergic and irreversible. The primary product, the formyl $Cp_2Ce(CHO)$, is a fascinating one because the net charge on the formyl fragment is −1 and both oxygen and carbon atoms carry charges of −0.7 and −0.2, respectively, so the formyl fragment is η^2-bonded to the metallocene fragment. The negative charge on the carbon atom is the key to understanding the polarization and therefore the heterolytic activation of H_2 as the formyl fragment is converted to the methoxy fragment. The activation energy for reaction of the formyl with CH_4 is about 15 kcal mol^{-1} higher than that with H_2 and this difference is traced to the difference in the acidity of CH_4 relative to H_2. This, in turn, suggests that the sigma-bond metathesis transition states in the specific case of an alkyl or hydride resemble the transition states in proton-transfer reactions, and they can be usefully viewed as such.

Experimental Details

General. All manipulations were performed in an inert atmosphere using standard Schenk and dry box techniques. All solvents were dried and distilled from sodium or sodium benzophenone ketyl. High purity CO gas was obtained from BOC and used without further purification. Infrared spectra were recorded on a Perkin-Elmer 283 spectrometer as Nujol mulls between CsI plates. NMR spectra were recorded on Bruker AV-300 or AV-400 spectrometers at 19 °C in the solvent specified. J-Young NMR tubes were used for all NMR tube experiments. Melting points were measured on a Thomas-Hoover melting point apparatus in sealed capillaries. Electron impact mass spectrometry and elemental analyses were performed by the microanalytical facility at the University of California, Berkeley. The abbreviation Cp′ is used for the 1,2,4-tri-*t*-butylcyclopentadienyl ligand. Samples for GCMS were prepared by adding a drop of H_2O, agitating, and allowing the sample to stand closed for 10 min. The samples were then dried over magnesium sulfate, filtered, and diluted 10-fold with hexane. A 1 mL sample was injected into a HP6890 GC system with a J&W DB-XLB universal nonpolar column, attached to an HP5973 Mass Selective Detector. The principle elution peaks consisted of hexane, free Cp′H and isomeric 1,2-bis-(trimethylsiloxy)ethylenes.

Cp'_2CeCl. Anhydrous $CeCl_3$ (1.0 g, 4.1 mmol, dried by heating at reflux in $SOCl_2$) and Cp'_2Mg[44] (1.99 g, 4.1 mmol) were stirred at reflux in a mixture of pyridine (5 mL) and toluene (50 mL) for 24 h. The yellow-brown suspension was taken to dryness under reduced pressure. The solid residue was extracted with toluene (50 mL). The volume of the solution was reduced until precipitation occurred, warmed to dissolve the precipitate, and then cooled to −15 °C, yielding yellow crystals. Yield: 1.1 g (1.7 mmol, 42%). MP 233−236 °C. ^{1}H NMR (C_6D_6, 300 MHz): δ −2.58 (36H, $\nu_{1/2}$ = 90 Hz), −13.3 (18H, $\nu_{1/2}$ = 80 Hz). MS $(M)^+$ *m*/*z* (calc, found) 641 (100, 100) 642 (37, 34) 643 (51, 50) 644 (17, 15) 645 (7, 6). Anal. Calcd for $C_{34}H_{58}CeCl$: C, 63.57; H, 9.10. Found C, 63.72; H, 9.37.

Cp'_2CeN_3. Cp'_2CeCl (0.8 g, 1.2 mmol) was dissolved in toluene (50 mL), and trimethylsilylazide (0.25 mL, 1.9 mmol) was added by syringe. The orange suspension was stirred at room temperature for 3 days. The solvent was removed under reduced pressure, the orange solid residue was suspended in toluene (50 mL), trimethylsilylazide (0.25 mL, 1.9 mmol) was added by syringe, and the suspension was stirred

(43) (a) Thompson, M. E.; Baxter, S. M.; Bulls, A. R.; Burger, B. J.; Nolan, M. C.; Santarsiero, B. D.; Schaefer, W. P.; Bercaw, J. E. *J. Am. Chem. Soc.* **1987**, *109*, 203. (b) McMillen, D. F.; Golden, D. M. *Ann. Rev. Phys. Chem.* **1982**, *33*, 493. Blanksby, S. J.; Ellison, G. B. *Acc. Chem. Res.* **2003**, *36*, 255.

(44) Weber, F.; Sitzmann, H.; Schultz, M.; Sofield, C. D.; Andersen, R. A. *Organometallics* **2002**, *21*, 3139.

at room temperature for three more days. This procedure was repeated once more, and the solvent was removed under reduced pressure. The orange solid residue was dissolved in toluene (200 mL), and the volume of the solution was reduced until precipitation occurred. The solution was warmed to dissolve the precipitate and cooled to −15 °C, yielding an orange powder. Yield, 0.4 g (0.6 mmol, 51%). MP 307−310 °C (dec with gas evolution). ^{1}H NMR (C_6D_6, 300 MHz): δ 3.09(18H, $\nu_{1/2}$ = 70 Hz), −4.11 (18H, $\nu_{1/2}$ = 50 Hz), −8.16 (18H, $\nu_{1/2}$ = 50 Hz). IR: 3505(w), 3435(w), 3090(w), 2240(w), 2130(s), 1590(w), 1390(w), 1365(s), 1245(s) 1210(w), 1200(w), 1170(m), 1030(w), 1005(m), 960(w), 825(s), 820(s), 780(w), 685(m), 675(m), 620(w), 600(w), 560(w) cm^{-1}. Anal. Calcd for $C_{34}H_{58}CeN_3$: C, 62.93; H, 9.01; N, 6.47. Found C, 63.11; H, 8.93; N, 6.58.

Cp′$_2$CeCH$_2$OCeCp′$_2$·Toluene, 2·Toluene. Cp′$_2$CeH (0.75 g, 1.2 mmol)[14a] was dissolved in pentane (5 mL), and the solution was chilled in an ice−water bath. The headspace was evacuated and replaced by CO (1 atm). The purple solution turned red orange, and a copious amount of yellow-orange solid precipitated. The solution was filtered, and the solid was dissolved in toluene (100 mL). The volume of the solution was reduced to 75 mL, and the solution was cooled to −15 °C, yielding small orange crystals. The crystals became opaque upon exposure to vacuum; the ^{1}H NMR spectrum indicated the presence of toluene as did the combustion analysis. Yield, 0.56 g (0.42 mmol, 70%). MP 211−215 °C (decomp). ^{1}H NMR (C_6D_{12}, 400 MHz): δ 8.95 (18H, $\nu_{1/2}$ = 17 Hz), −3.38 (18H, $\nu_{1/2}$ = 17 Hz), −15.62 (18H, $\nu_{1/2}$ = 31 Hz). IR: 2130(m),[45] 1520(w), 1360(s), 1240(s), 1200(m), 1180(m), 1160(m), 1110(w), 1020(w), 1000(m), 960(m), 920(w), 880(w), 825(w), 810(w), 800(s), 760(w), 720(w), 680(m), 675(m) cm^{-1}. MS: no (M)$^+$ was observed but (M-605)$^+$ corresponding to Cp′$_2$CeOMe and (M-636)$^+$ corresponding to Cp′[(Me$_3$C)$_2$C$_5$H$_2$C(Me$_2$)CH$_2$]Ce were found. Anal. Calcd for $C_{76}H_{118}Ce_2O$: C, 68.32; H, 9.50. Found C, 68.65; H, 9.59. The crystallographic details are included as Supporting Information.

Cp′$_2$CeOMe, 3. Method A: Cp′$_2$CeH (0.5 g, 0.8 mmol) was dissolved in pentane (10 mL). The headspace was evacuated and replaced with a 10:1 mixture of H_2 and CO (1 atm). The solution became cloudy but gradually cleared over 6 h. The headspace was again evacuated and replaced with a 10:1 mixture of H_2 and CO (1 atm). After 12 h, the volume of the solution was reduced to 2 mL, and the solution was cooled to −15 °C, yielding red powder. Yield, 0.12 g (0.18mmol, 23%). Melts over a wide range, about 150 °C. ^{1}H NMR (C_6D_6, 300 MHz): δ 31.04 (3H, $\nu_{1/2}$ = 18 Hz), 23.33 (4H, $\nu_{1/2}$ = 55 Hz), −2.51 (36H, $\nu_{1/2}$ = 11 Hz), −8.62 (18H, $\nu_{1/2}$ = 15 Hz). MS (M)$^+$ *m*/*z* (calc, found) 637 (100, 100) 638 (38, 48) 639 (20, 24) 640 (6, 8) 641 (1, 3). Anal. Calcd for $C_{35}H_{61}CeO$: C, 65.89; H, 9.63. Found C, 66.17; H, 9.71. The above synthetic route was the only one that gave pure methoxide; products from reaction of Cp′$_2$CeCH$_2$Ph and methanol or Cp′$_2$CeOTf and NaOMe could not be purified.

Cp′$_2$Ce^{18}OMe, 3-^{18}O. Cp′$_2$CeH (0.5 g, 0.8 mmol) was dissolved in C_6D_{12} in an NMR tube. The sample was chilled in a liquid nitrogen isopropanol bath. The headspace was evacuated and replaced by C^{18}O (1 atm). The sample was warmed to room temperature and agitated, producing copious quantities of yellow-orange precipitate. The suspension was returned to the liquid nitrogen isopropanol bath, the headspace was evacuated and replaced with H_2 (1 atm). The sample was warmed to room temperature and agitated until all of the solid had dissolved. The EI mass spectrum indicated the presence of Cp′$_2$Ce^{18}OMe. The presence of Cp′$_2$CeOMe was not detected. MS (M)$^+$ *m*/*z* (calc, found) 639 (100, 100) 640 (38, 37) 641 (20, 20) 642 (6, 3).

NMR Tube Reaction of Cp′$_2$CeCH$_2$OCeCp′$_2$ with H$_2$. Cp′$_2$CeCH$_2$OCeCp′$_2$ was dissolved in C_6D_6. The sample was cooled in a liquid nitrogen isopropanol bath; the headspace was evacuated, and replaced with H_2 (1 atm). After 4 h, the ^{1}H NMR spectrum contained only resonances due to Cp′$_2$CeOMe and Cp′$_2$CeH in an area ratio of approximately 1:1.

***cis*-Cp′$_2$CeOCHCHOCeCp′$_2$, 1-cis.** Cp′$_2$CeH (0.5 g, 0.8 mmol) was dissolved in toluene (20 mL). The headspace was evacuated and replaced by CO (1 atm). The purple solution turned red orange and became cloudy. After 20 min, the solution had become clear and red. The headspace was evacuated and replaced with CO (1 atm). After stirring for 1 h, the solvent was removed under reduced pressure. The red solid residue was dissolved in pentane (10 mL). The volume of the solution was reduced until precipitation occurred; the solution was warmed to dissolve the solid, and then cooled to −15 °C, yielding a red powder. Yield, 0.28 g (0.22 mmol, 55%). MP 232−235 °C. ^{1}H NMR (C_7D_8, 400 MHz): δ 39.33 (2H, $\nu_{1/2}$ = 80 Hz), 26.94 (4H, $\nu_{1/2}$ = 450 Hz), −0.73 (36H, $\nu_{1/2}$ = 550 Hz), −12.53 (18H, $\nu_{1/2}$ = 100 Hz). IR: 2130(w),[45] 1700(w), 1650(w), 1620(s), 1590(w), 1570(w), 1360(s), 1330(m), 1280(w), 1240(s), 1200(m), 1160(m), 1140(s), 1060(w), 1020(s), 1000(m), 960(m), 920(w), 820(s), 800(s), 760(w), 740(w), 720(w), 680(w), 670(m) cm^{-1}. MS (M)$^+$ *m*/*z* (calc, found) 1270 (100, 100) 1271 (77, 76) 1272 (55, 54) 1273 (27, 27) 1274 (10, 14). Anal. Calcd for $C_{70}H_{118}Ce_2O_2$: C, 66.10; H, 9.35. Found C, 66.00; H, 9.43. Full crystallographic details are included in the Supporting Information. Triclinic cell, Space Group, $P\bar{1}$: a = 12.280(12) Å, b = 16.117(16) Å, c = 19.427(18) Å, α = 84.98(2)°, β = 79.55(2)°, γ = 68.33(2)°, V = 8876(1) Å.^{3}

***trans*-Cp′$_2$CeOCHCHOCeCp′$_2$, 1-trans.** Method A: *cis*-Cp′$_2$CeOCH$_2$CH$_2$OCeCp′$_2$ was dissolved in C_7D_8 in an NMR tube, and the sample was heated at 97 °C in an oil bath. After 2 days, new resonances ascribed to *trans*-Cp′$_2$CeOCH$_2$CH$_2$OCeCp′$_2$ appeared in the ^{1}H NMR spectrum. The cis to trans ratio was 24:1. After 63 days, the ratio was 1:2.5. After 200 days, only resonances due to *trans*-Cp′$_2$CeOCH$_2$CH$_2$OCeCp′$_2$ remained in the spectrum. ^{1}H NMR (C_7D_8, 300 MHz): δ 35.26 (2H, $\nu_{1/2}$ = 20 Hz), 26.72 (4H, $\nu_{1/2}$ = 70 Hz), −1.39 (36H, $\nu_{1/2}$ = 20 Hz), −8.17(18H, $\nu_{1/2}$ = 30 Hz).

Method B: *cis*-Cp′$_2$CeOCH$_2$CH$_2$OCeCp′$_2$ was sealed in an ampule under vacuum and heated to 220 °C in a sand bath. After 45 days, small, light orange crystals of *cis*-Cp′$_2$CeOCH$_2$CH$_2$OCeCp′$_2$ and larger, deep red crystals of *trans*-Cp′$_2$CeOCH$_2$CH$_2$OCeCp′$_2$ had formed on the glass walls of the ampule.

Full crystallographic details are included in the Supporting Information. Triclinic cell, Space Group $P\bar{1}$: a = 10.5543(6) Å, b = 10.6580(6) Å, c = 15.7061(9) Å, α = 73.949(1)°, β = 81.190(1)°, γ = 83.217(1)°, V = 1672.5(2) Å^3.

NMR Reaction of Cp′$_2$CeCH$_2$OCeCp′$_2$, 2, with CO. Cp′$_2$CeCH$_2$OCeCp′$_2$ was dissolved in C_7D_8, and the sample was cooled in a liquid nitrogen isopropanol bath. The headspace was evacuated and replaced with CO (1 atm). The orange solution became more red upon agitation. The ^{1}H NMR spectrum showed the formation of *cis*-Cp′$_2$CeOCHCHOCeCp′$_2$ and Cp′$_2$CeOMe in a 9:1 ratio.

NMR Tube Reaction of Cp′$_2$CeH, CH$_4$, and CO. Cp′$_2$CeH was dissolved in C_6D_6 and the sample was cooled in a liquid nitrogen isopropanol bath. The headspace was evacuated and replaced with CH_4 (1 atm). The headspace was evacuated to roughly 0.5 atm and replaced with CO (1 atm). The sample was warmed to room temperature and agitated, and it became red orange and cloudy. After 1 day, the sample was red and clear. The ^{1}H NMR spectrum contained resonances due to *cis*-Cp′$_2$CeOCHCHOCeCp′$_2$ and a small amount of Cp′$_2$CeOMe. The presence of CH_4 did not appear to affect the course of the reaction.

Decomposition of Cp′$_2$CeCH$_2$OCeCp′$_2$, 2, in C$_6$D$_{12}$. Cp′$_2$CeCH$_2$OCeCp′$_2$ was dissolved in C_6D_{12}, and the sample was monitored by ^{1}H NMR spectroscopy. After 7.5 h, resonances due to Cp′$_2$CeOMe and Cp′[(Me$_3$C)$_2$C$_5$H$_2$C(Me$_2$)CH$_2$]Ce had appeared in the ^{1}H NMR spectrum and the resonances due to Cp′$_2$CeCH$_2$OCeCp′$_2$ had diminished relative to an internal standard. The area ratio of the resonances due to Cp′$_2$CeOMe and Cp′$_2$CeCH$_2$OCeCp′$_2$ was 1:1. After 12 h, the ratio had changed to 5:1. After 24 h, only resonances due to Cp′$_2$CeOMe and Cp′[(Me$_3$C)$_2$C$_5$H$_2$C(Me$_2$)CH$_2$]Ce were present in the spectrum.

(45) This absorbance was attributed to an electronic transition arising from the split ^{2}F ground state of Ce^{3+}, ($^2F_{5/2}$ and $^2F_{3/2}$); Heeres, H. J.; Renkema, J.; Booij, M.; Meetsma, A.; Teuben, J. H. *Organometallics* **1988**, *7*, 2495.

NMR Tube Reaction of $Cp'_2CeCH_2OCeCp'_2$, 2, and $(Cp'\text{-}d_{27})_2CeCH_2OCe(Cp'\text{-}d_{27})_2$, 2-$d_{108}$, with CO. Cp'_2CeH was dissolved in C_6D_6 and heated at 60 °C for 4 days to perdeuterate the ring *t*-butyl groups. The sample was taken to dryness and the solid residue was dissolved in fresh C_6D_6. The sample was heated for an additional 4 days, yielding a solution of $(Cp'\text{-}d_{27})CeD$. The tube was cooled in a liquid nitrogen isopropanol bath, the head space was evacuated, and replaced with CO (1 atm). The sample was warmed to room temperature and agitated for 30 s, producing copious quantities of yellow-orange precipitate. The sample was taken to dryness. Another sample of Cp'_2CeH was dissolved in C_6D_6, cooled in a liquid nitrogen isopropanol bath, the head space was evacuated, and replaced with CO (1 atm). The sample was warmed to room temperature and agitated for 30 s, producing copious quantities of yellow-orange precipitate. The sample was taken to dryness. The two samples were suspended in C_7D_8 and combined. The mixed sample was cooled in a liquid nitrogen isopropanol bath, the headspace was evacuated, and replaced with CO (1 atm). The sample was warmed to room temperature and agitated until all precipitate had dissolved. The solution was taken to dryness, yielding a red solid. The EI mass spectrum contained envelopes centered at *m*/*z* 1272, 1299, 1326, 1353, and 1380, suggesting the formation of $Cp'_2CeOC(H,D)C(H,D)OCeCp'_2$, $Cp'(Cp'\text{-}d_{27})CeOC(H,D)C(H,D)OCeCp'_2$, $(Cp'\text{-}d_{27})_2CeOC(H,D)C(H,D)OCeCp'_2$, $(Cp'\text{-}d_{27})_2CeOC(H,D)C(H,D)OCe(Cp'\text{-}d_{27})Cp'$, and $(Cp'\text{-}d_{27})_2CeOC(H,D)C(H,D)OCe(Cp'\text{-}d_{27})_2$.

NMR Tube Reaction of *cis*-$Cp'_2CeOCHCHOCeCp'_2$, 1-*cis*, and *cis*-$(Cp'\text{-}d_{27})_2CeOCHCHOCe(Cp'\text{-}d_{27})_2$, 1-*cis*-$d_{108}$. Cp'_2CeH was dissolved in C_6D_6 and heated at 60 °C for 4 days to perdeuterate the ring t-butyl groups. The sample was taken to dryness and the solid residue redissolved in fresh C_6D_6. The sample was heated for an additional 4 days, yielding a solution of $(Cp'\text{-}d_{27})CeD$. The tube was cooled in a liquid nitrogen isopropanol bath, the head space was evacuated, and replaced with CO (1 atm). The sample was warmed to room temperature and agitated until all precipitate had dissolved. Another sample of Cp'_2CeH was dissolved in C_6D_6, cooled in a liquid nitrogen isopropanol bath, the head space was evacuated, and replaced with CO (1 atm). The sample was warmed to room temperature and agitated until all precipitate had dissolved. The two samples were combined and heated at 60 °C for 12 h, then taken to dryness, yielding a red solid. The EI mass spectrum contained envelopes centered at *m*/*z* 1272, 1299, 1326, 1353, and 1380, suggesting the formation of $Cp'_2CeOC(H,D)C(H,D)OCeCp'_2$, $Cp'(Cp'\text{-}d_{27})CeOC(H,D)C(H,D)OCeCp'_2$, $(Cp'\text{-}d_{27})_2CeOC(H,D)C(H,D)OCeCp'_2$, $(Cp'\text{-}d_{27})_2CeOC(H,D)C(H,D)OCe(Cp'\text{-}d_{27})Cp'$, and $(Cp'\text{-}d_{27})_2CeOC(H,D)C(H,D)OCe(Cp'\text{-}d_{27})_2$.

NMR Tube Reaction of $Cp'_2CeCH_2OCeCp'_2$, 2, and ^{13}CO. Cp'_2CeH was dissolved in C_6D_{12}. The tube was cooled in a liquid nitrogen isopropanol bath, the head space was evacuated and replaced with CO (1 atm). The sample was warmed to room temperature and agitated for 30 s, producing copious quantities of yellow-orange precipitate. The tube was cooled in a liquid nitrogen isopropanol bath, the head space was evacuated, and replaced with ^{13}CO (1 atm). The sample was warmed to room temperature and agitated until all precipitate had dissolved. The sample was taken to dryness, yielding a red solid. The EI mass spectrum contained an envelope whose intensity pattern suggested the presence of $Cp'_2CeOCH_2CH_2OCeCp'_2$, $Cp'_2CeO^{13}CH_2CH_2OCeCp'_2$, and $Cp'_2CeO^{13}CH_2{}^{13}CH_2OCeCp'_2$. MS *m*/*z* (rel. intensity found) 1270 (10), 1271 (76), 1272 (100), 1273 (63), 1274 (2).

NMR Tube Reaction of $Cp'_2CeCH_2{}^{18}OCeCp'_2$, 2-$^{18}O$, and CO. Cp'_2CeH was dissolved in C_6D_{12}. The tube was cooled in a liquid nitrogen isopropanol bath, the head space was evacuated, and replaced with $C^{18}O$ (1 atm). The sample was warmed to room temperature and agitated for 30 s, producing copious quantities of a yellow-orange precipitate. The tube was cooled in a liquid nitrogen isopropanol bath, the head space was evacuated, and replaced with CO (1 atm). The sample was warmed to room temperature and agitated until all of the precipitate had dissolved. The sample was taken to dryness, yielding a red solid. The EI mass spectrum contained an envelope whose most intensity pattern was consistent with the formation of $Cp'_2CeOCH_2CH_2OCeCp'_2$, $Cp'_2Ce^{18}OCH_2CH_2OCeCp'_2$, and $Cp'_2Ce^{18}OCH_2CH_2{}^{18}OCeCp'_2$. MS *m*/*z* (rel. intensity found) 1270 (19), 1271 (14), 1272 (90), 1273 (66), 1274 (100), 1275 (63), 1276 (38), 1277 (17), 1278 (6) 1279 (1). Thus, fragmentation occurs in the mass spectrometer. The experiment was repeated, but after the sample was warmed to room temperature and all of the precipitate had dissolved, an excess of trimethylsilylazide was added, the sample was agitated, and the resulting orange suspension was allowed to settle. The ^1H NMR spectrum indicated the formation of Cp'_2CeN_3, *cis*-1,2-$(Me_3SiO)_2C_2H_2$, and a small amount of *trans*-1,2-$(Me_3SiO)_2C_2H_2$.[17] Analysis by GCMS showed one major component in addition to Cp′H with $(M)^+$ *m*/*z* 206, corresponding to the cis isomer of $Me_3SiOCHCH^{18}OSiMe_3$. The isotope pattern indicated the presence of approximately 4% $Me_3Si^{18}OCHCH^{18}OSiMe$ but no $Me_3SiOCHCHOSiMe$ in the product distribution. GCMS $(M)^+$ *m*/*z* (calc, found) 206 (100, 100) 207 (19, 18) 208 (9, 12), 209 (1, 3). Thus, the bissiloxyethenes do not fragment in the mass spectrometer.

NMR Tube Reaction of *cis*-$Cp'_2CeOCHCHOCeCp'_2$ and *cis*-$Cp'_2Ce^{18}OCHCH^{18}OCeCp'_2$. Cp'_2CeH was dissolved in C_6D_{12}. The tube was cooled in a liquid nitrogen isopropanol bath, the head space was evacuated, and replaced with CO (1 atm). The sample was warmed to room temperature and agitated until all of the precipitate had dissolved. Another sample of Cp'_2CeH was dissolved in C_6D_6, cooled in a liquid nitrogen isopropanol bath, the head space was evacuated, and replaced with $C^{18}O$ (1 atm). The sample was warmed to room temperature and agitated until all of the precipitate had dissolved. The two samples were taken to dryness and approximately equal portions of the dark-red solids were mixed. The EI mass spectrum contained an envelope whose intensity pattern suggested the formation of $Cp'_2CeOCH_2CH_2OCeCp'_2$, $Cp'_2Ce^{18}OCH_2CH_2OCeCp'_2$, and $Cp'_2Ce^{18}OCH_2CH_2{}^{18}OCeCp'_2$. MS *m*/*z* (rel. intensity found) 1270 (100), 1271 (70), 1272 (64), 1273 (35), 1274 (34), 1275 (18), 1276 (11), 1277 (5), 1278 (2), and therefore scrambling occurred.

NMR Tube Reaction of *cis*-$Cp'_2Ce^{18}OCHCH^{18}OCeCp'_2$, 1-*cis*-$(^{18}O)_2$, and CO. Cp'_2CeH was dissolved in C_6D_{12}.The tube was cooled in a liquid nitrogen isopropanol bath, and the head space was evacuated and replaced with $C^{18}O$ (1 atm). The sample was warmed to room temperature and agitated until all of the precipitate had dissolved, yielding a red solution. The sample was divided into two portions. One portion was returned to the liquid nitrogen isopropanol bath, and the headspace was evacuated and replaced with CO (1 atm). Both samples were stored at room temperature for 2 days. An excess of trimethylsilylazide was added to both samples, and the resulting orange suspensions were allowed to settle. The ^1H NMR spectra indicated the formation of Cp'_2CeN_3, *cis*-1,2-$(Me_3SiO)_2C_2H_2$, and a small amount of *trans*-1,2-$(Me_3SiO)_2C_2H_2$ in both cases. Analysis by GCMS showed two major components in each sample in addition to Cp′H, all with $(M)^+$ *m*/*z* 208 and identical isotope patterns corresponding to the cis and trans isomers of $Me_3Si^{18}OCHCH^{18}OSiMe_3$. No $Me_3SiOCHCH^{18}OSiMe_3$ nor $Me_3SiOCHCHOSiMe_3$ were observed in any of the isotope patterns. Typical isotope pattern: GCMS $(M)^+$ *m*/*z* (calc, found) 208 (100, 100) 209 (19, 23) 210 (9, 9), 211 (1, 2).

NMR Tube Reaction of *cis*-$Cp'_2CeO^{13}CH^{13}CHOCeCp'_2$, 1-*cis*-$(^{13}C)_2$, and CO. Cp'_2CeH was dissolved in C_7D_8. The tube was cooled in a liquid nitrogen isopropanol bath, the head space was evacuated, and replaced with ^{13}CO (1 atm). The sample was warmed to room temperature and agitated until all of the precipitate had dissolved, yielding a red solution. The ^1H NMR spectrum was identical to that of *cis*-$Cp'_2CeOCH_2CH_2OCeCp'_2$ except that the resonance at $\delta = 39$ ppm, corresponding to the two olefinic protons, was a broadened doublet, $^2J_{HC} = 180$ Hz. The sample was returned to the liquid nitrogen isopropanol bath, the headspace was evacuated, and replaced with CO (1 atm). The sample was heated at 60 °C for 62 days; the ratio of *cis*- to *trans*-

$Cp'_2CeO^{13}CH^{13}CHOCeCp'_2$ was 1:4. The broadened doublet corresponding to the olefinic protons of the trans isomer, $\delta = 35.3$ ppm ($^2J_{HC} = 190$ Hz), was symmetric. An excess of trimethylsilylazide was added, the sample was agitated, and the resulting orange suspension was allowed to settle. The ^{1}H NMR spectrum indicated the formation of Cp'_2CeN_3, *cis*-1,2-$(Me_3SiO)_2C_2H_2$, and *trans*-1,2-$(Me_3SiO)_2C_2H_2$. Analysis by GCMS showed two major components in addition to Cp′H with $(M)^+$ *m*/*z* 206 and identical isotope patterns corresponding to the cis and trans isomers of $Me_3SiO^{13}CH^{13}CHOSiMe_3$. No $Me_3SiOCHCHOSiMe_3$ nor $Me_3SiOCH^{13}CHOSiMe_3$ were observed in either of the isotope patterns. Typical isotope pattern: GCMS $(M)^+$ *m*/*z* (calc, found) 206 (100, 100) 207 (19, 30) 208 (9, 11).

Computational Details

The Stuttgart-Dresden-Bonn large core Relativistic Effective Core Potential (RECP)[46] has been used to represent the inner shells of Ce. The associated basis set augmented by an f polarization function ($\alpha = 1.000$) has been used to represent the valence orbitals. C, O, and H have been represented by an all-electron 6-31G(d, p) basis set.[47] Calculations have been carried out at the DFT(B3PW91) level[48] with Gaussian 98.[49] The nature of the extrema (minimum or transition state) has been established with analytical frequencies calculations and the intrinsic reaction coordinate (IRC) has been followed to confirm that transition states connect to reactants and products. The zero point energy (ZPE) and entropic contribution have been estimated within the harmonic potential approximation. The Gibbs free energy, ΔG, was calculated for $T = 298.15$ K and 1 atm. The NBO analysis[50] was carried out replacing Ce by La because of the technical requirement to have even number of f electrons for the calculations. Following the tradition, we report geometrical parameters with an accuracy of 10^{-3} Å and angles with an accuracy of 10^{-1} degrees although we often discuss the geometrical parameters with lesser accuracy because of the many approximations made in the modeling and in the level of calculation.

(46) Dolg, M.; Stoll, H.; Savin, A.; Preuss, H. *Theor. Chim. Acta* **1989**, *75*, 173. Dolg, M.; Stoll, H.; Preuss, H. *Theor. Chim. Acta* **1993**, *85*, 441.
(47) Hariharan, P. C.; Pople, J. A. *Theor. Chim. Acta* **1973**, *28*, 213.
(48) Perdew, J. P.; Wang, Y. *Phys. Rev. B*, 1992, **45**, 13244. Becke, A. D. *J. Chem. Phys.* **1993**, *98*, 5648. Burke, K.; Perdew, J. P.; Yang, W. In *Electronic Density Functional Theory: Recent Progress and New Directions*; Dobson, J. F., Vignale, G., Das, M. P., Eds.; Plenum: New York, 1998.
(49) Pople, J. A.; et al. *Gaussian 98*, revision A.9; Gaussian, Inc.: Pittsburgh, PA, 1998.
(50) Reed, A. E.; Curtiss, L. A.; Weinhold, F. *Chem. Rev.* **1988**, *88*, 899.

Acknowledgment. This work was partially supported by the Director Office of Energy Research Office of Basic Energy Sciences, Chemical Sciences Division of the U.S. Department of Energy under Contract No DE-AC02-05CH11231. X-ray intensity data for **1-cis** were collected at beam line 11.3.1 at the Advanced Light Source at LBNL under DOE contract No DE-AC03-76SF00098. Calculations were in part carried out on the national computing centers CINES and CALMIP (France). O.E. thanks the Miller Institute for a Visiting Miller Professorship at U.C. Berkeley. The French authors thank the CNRS, notably the PICS 3422, and the Ministère of National Education for funding. We thank Dr. Fred Hollander and Dr. Allen Oliver for their assistance with the crystallography (at CHEXRAY the U.C. Berkeley X-ray diffraction facility). We thank Dr. Eric Clot (CTMM, Institut Charles Gerhardt, Université Montpellier 2) for help in the calculations of the conformations preference and hydrogenation energies of the models enediolates species.

Supporting Information Available: Complete ref 49; list of energies (*E*), Gibbs free energies (*G*) in a.u., and coordinates of all calculated systems; X-ray crystallographic data (CIF).This material is available free of charge via the Internet at http://pubs.acs.org. Crystallographic data for the structures in this paper have also been deposited with the Cambridge Crystallographic Data Center. Copies of the data (CCDC 280947 for *trans*-$Cp'_2CeOCH_2CH_2OCeCp'_2$, CCDC 618063 for *cis*-$Cp'_2CeOCH_2CH_2OCeCp'_2$, CCDC 280948 for $Cp'_2CeCH_2OCeCp'_2$) can be obtained free of charge via www.ccdc.cam.ac.uk/data_request/cif, by emailing data_request@ccdc.cam.ac.uk, or by contacting The Cambridge Crystallographic Data Center, 12 Union Road, Cambridge CB2 1EZ, UK; fax +44 1223 336033.

JA066482H